Plant Physiology and Biochemistry 140 (2019) 27–42

Contents lists available at ScienceDirect

Plant Physiology and Biochemistry

journal homepage: www.elsevier.com/locate/plaphy

Research article

Zinc priming and foliar application enhances photoprotection mechanisms in drought-stressed wheat plants during anthesis

Ivo Pavia[a], João Roque[c], Luís Rocha[a], Helena Ferreira[a], Cláudia Castro[c], Ana Carvalho[a,b,c], Ermelinda Silva[a], Cátia Brito[a], Alexandre Gonçalves[a], José Lima-Brito[a,b,c], Carlos Correia[a,*]

[a] CITAB - Centre for the Research and Technology of Agro-Environmental and Biological Sciences, Universidade de Trás-os-Montes e Alto Douro, Quinta de Prados, 5000-801, Vila Real, Portugal
[b] Universidade de Trás-os-Montes e Alto Douro, Quinta de Prados, 5000-801, Vila Real, Portugal
[c] BioISI – UTAD, Biosystems & Integrative Sciences Institute - Universidade de Trás-os-Montes e Alto Douro, Quinta de Prados, 5000-801, Vila Real, Portugal

ARTICLE INFO

Keywords:
Heat dissipation
Photosynthesis
Recovery
Triticum aestivum
Y_{NO}
Y_{NPQ}

ABSTRACT

Drought is one of most important limiting factors in wheat productivity worldwide. The need to increase drought tolerance during anthesis is of the utmost importance for high yield potentials and yield stability. Photosynthesis is one of the major physiological processes affected by drought. Damages in the photosynthetic apparatus may also arise due to non-regulated dissipation of excessive energy. Zinc (Zn) is an indispensable micronutrient for plants and is required for a wide range of physiological and biochemical processes. In this work we evaluated the stress mitigation effects of Zn seed priming alone and coupled with Zn foliar application in wheat plants submitted to severe drought during anthesis, followed by a recovery period. Under such severe drought stress, photosynthesis was constrained by both stomatal and non-stomatal limitation. Severe drought also induced an increase in non-regulated energy dissipation and hindered a full recovery of the plant's photosynthetic processes after rewatering. We also report possible activation of transposable elements due to drought stress and Zn application. Yield was severely decreased by drought and Zn treatments were unable to counteract this effect. Although unable to oppose the reduction of net photosynthesis, Zn treatments positively enhance photoprotection. At the end of drought period, Zn priming alone and coupled with Zn foliar application increased, respectively, over 2- and 3- fold the regulated dissipation of excess energy. Zn treatments lessened the non-regulated energy dissipation caused by drought, protected the plants against irreversible damages to the photosynthetic apparatus and enabled a better recovery of wheat plants after stress relief.

1. Introduction

Wheat (*Triticum* spp.) is one of the most important crops worldwide. This crop occupies 22% of the global cultivated area (Leff et al., 2004) and is a critical component of the diet of approximately 2.5 billion people (Shiferaw et al., 2013).

Environmental factors, such as water availability and temperature, highly affect wheat yield (Semenov et al., 2014; Zhang et al., 2018). One of the most important limiting factors in cereal productivity worldwide is drought (Daryanto et al., 2016; Lesk et al., 2016; Zhang et al., 2018). Recent meta-analysis showed that drought is able to decrease, on average, wheat yield by 20–30% (Daryanto et al., 2016; Zhang et al., 2018).

In Mediterranean regions, rain falls mostly during autumn and winter. Consequently, water deficit rises in spring, coinciding with the anthesis and grain filling period of wheat (Acevedo et al., 1999). Although drought can affect plant growth at any time from sowing to grain maturity, heading/anthesis and grain filling are considered critical periods for yield determination (Otegui and Slafer, 2004; Barnabás et al., 2007; Zhang et al., 2018). Drought during heading/anthesis may lead to a reduction in grain number while at grain filling leads to a decrease in average grain weight (Otegui and Slafer, 2004; Barnabás et al., 2007; Dolferus et al., 2011; Zhang et al., 2018). Comparing the two periods, anthesis is considered to be the most critical stage, as the cereal yield is more closely related to the number of grains than to the average grain weight (Barnabás et al., 2007). The need to increase drought tolerance during reproductive development is of the utmost importance for high yield potentials and greater yield stability of wheat under climate change in Europe (Senapati et al., 2018).

* Corresponding author.
E-mail address: ccorreia@utad.pt (C. Correia).

https://doi.org/10.1016/j.plaphy.2019.04.028
Received 25 January 2019; Received in revised form 18 March 2019; Accepted 21 April 2019
Available online 02 May 2019

The severity and duration of stress events determine the extent of the yield loss. As reviewed by Farooq et al. (2014), drought during reproductive and grain-filling phases induces pollen sterility, accelerates leaf senescence, increases oxidative damage in the photo-assimilatory machinery and reduces the rate of carbon fixation. As such, photosynthesis is one of the major and more important physiological processes affected by drought (Farooq et al., 2009; Zargar et al., 2017). Reduction of the CO_2 assimilation, lower stomatal conductance and reduction of the quantum yield of photosystem II (PSII) are the main consequence of drought which affect photosynthesis (Lu and Zhang, 1999; Flexas and Medrano, 2002; Jaleel et al., 2009). Damage to the photosynthetic apparatus may also arise due to the generation of reactive oxygen species (ROS) by abiotic stress and by the absorption of excessive sunlight by the light-harvesting complex (Gururani et al., 2015; Zargar et al., 2017).

Moreover, drought and other abiotic stresses generate various genetically and epigenetically programmed responses (Chinnusamy and Zhu, 2009; Boyko and Kovalchuk, 2011; Luo et al., 2012), as well as genomic instability or remodelling (Alzohairy et al., 2014; Negi et al., 2016). The genomic instability arises from the responses of plant genomes to stress through transcriptional and transpositional activation of transposable elements (TEs), structural and sequence changes, alterations in the expression and regulation of affected genes, among others (Grandbastien, 1998, 2015; Huang et al., 2012; Alzohairy et al., 2014; Makarevitch et al., 2015; Negi et al., 2016).

Zinc (Zn) is recognized as an indispensable micronutrient for plants and a component of over 300 plant enzymes and vital proteins (Vallee and Falchuk, 1993; Laity et al., 2001). This micronutrient is required for a wide range of physiological and biochemical processes such as photosynthesis, protein synthesis, antioxidant function, pollination, and growth regulation (Römheld and Marschner, 1991; Brown et al., 1993; Cakmak, 2005; Hafeez et al., 2013). Agronomic biofortification by seed priming and foliar application with Zn was shown to increase wheat yield and alleviate the negative effects of drought (Yilmaz et al., 1997; Karim et al., 2012; Rehman et al., 2015; Ma et al., 2017). In addition, priming seeds in Zn-containing solutions were shown to increase Zn content in the primed seeds and/or to contribute to a better seedling growth and yield (Yilmaz et al., 1997; Harris et al., 2007; Rehman et al., 2015). Nonetheless, solutions with high Zn concentration may also be cytotoxic and impair plant growth (Rehman et al., 2015; Reis et al., 2018). Apart of re-establishing Zn concentration in Zn deficient seeds, the mechanism by which Zn priming enables this enhanced growth and yield are still to be explored. Recently, seed osmopriming was shown to be able to enhance photosynthesis and quantum yield in developed plants, leading to increased resistance to drought (Abid et al., 2018b). Meanwhile, the effects of foliar application are heavily dependent on the time of application (Ozturk et al., 2006; Cakmak, 2008; Velu et al., 2014). While foliar application at joining increased plant growth and grain yield (Hussain et al., 2012), foliar application during grain development was shown to mainly increase Zn concentration in the grain (Zhang et al., 2010; Hussain et al., 2012; Gomez-Coronado et al., 2016). Zn foliar application was also shown to alleviate drought stress in winter wheat (Karim et al., 2012; Ma et al., 2017). Application of Zn, Boron (B), and Manganese (Mn), at booting to anthesis, reduced the harmful effects of drought stress by increasing the rate of photosynthesis, pollen viability, number of fertile spikes, number of grains per spike, and particularly water-use efficiency (Karim et al., 2012). However, these authors suggest that the reported benefits may be due to control plants present micronutrient deficiencies which were surpassed by the application of the foliar spray. Ma et al. (2017) showed that foliar application of Zn alleviated wheat plant drought stress by Zn-mediated increase in photosynthetic pigments and active oxygen scavenging substances, and reduction in lipid peroxidation.

In this work, we aim to evaluate possible mitigation effects of stress using seed Zn priming and seed priming coupled with Zn foliar application in wheat plants submitted to drought during heading/anthesis. As far as we know, this is the first study which aims to assess possible changes in the physiological responses of Zn primed seeds. Furthermore, most of the reported studies suggest that the benefits of Zn priming and Zn foliar application may be due to micronutrient reestablishment in the crops (Yilmaz et al., 1997; Cakmak, 2005; Karim et al., 2012; Hussain et al., 2012). Therefore, previous research lack intentional focus on the responsible mechanism that may allow for better growth and yield under stress conditions. We hypothesise that Zn priming and Zn foliar application induce physiological changes which allows plants to deal with the harmful consequences of drought. To address this matter, the consequences of drought and Zn treatments were assessed regarding (1) leaf gas exchange; (2) chlorophyll *a* fluorescence; (3) leaf structure and water status; (4) foliar pigments; (5) genomic stability; and (6) yield.

2. Material and methods

2.1. Plant material and experimental design

In this work, we used seeds of plants of bread wheat (*Triticum aestivum* L.) cv 'Jordão' kindly given by Eng. Coutinho (INIAV-Elvas). This cultivar is registered on the Portuguese Catalogue of Varieties (CNV, 2018) and in the European Commission's Plant Variety Database (EUPVD). It presents an excellent adaptation to Mediterranean conditions, semi-precocious vegetative cycle, great tillering capacity, high productive performance, high baking potential, and high resistance against several wheat diseases.

The experiment was carried out at the experimental greenhouses of the University of Trás-os-Montes e Alto Douro, Portugal (41°16′54″N, 7°44′41″W) between December of 2015 and July of 2016.

A total of 90 pots were used. Circular pots, with 20 cm of diameter and 23 cm of height, were filled with soil. The soil was collected at "Quinta de Prados", University of Trás-os-Montes e Alto Douro, Portugal (41°16′54″N, 7°44′41″W). The soil presented gross texture, pH (in water) of 5.2, 1.4% organic matter, 48 mg P_2O_5 Kg^{-1}, and 130 mg K_2O Kg^{-1}.

Seeds of bread wheat cv. 'Jordão' were submerged (primed) in a $ZnSO_4$-heptahydrate solution with 0.4% Zn for 8 h. Control seeds were submerged in distilled water for 8 h. Seeds were then air dried. Initially, 6 seed were sown per pot (Day 0). Later, 4 plants were maintained per pot after 2 weeks of germination. A total of 30 pots were sown with control seeds and 60 with Zn primed seeds. In the beginning, the pots were kept outside and the plants in rainfed conditions. Monthly average temperatures and accumulated precipitation at the trial site are available in Fig. S1. All pots were transferred to a greenhouse at the end of April (Day 140). A $ZnSO_4$-heptahydrate solution with 0.1% Zn and 0.1% Tween was applied as foliar spray the following day, during booting (Feekes 10), on 30 plants previously primed with 0.4% Zn. The 0.1% Zn solution was applied until the plants leaves surface were covered/saturated (*c.a.* 25 mL of solution per vase). This was achieved with pressurized manual foliar sprayer. Summarily, two distinct Zn treatments were applied: zinc priming (ZP) and zinc priming plus foliar application (ZPF). Plants where no treatment was applied were denominated as control (C). For each treatment, during heading (Feekes 10.1) and anthesis (Feekes 10.5.3), a group of 15 pots was submitted to 20 consecutive days of drought stress (water-stressed - WS), where volumetric soil water content was maintained at 5%, while another group of 15 pots was kept in good water status (well-watered - WW), with 20% soil humidity. Soil moisture was regularly checked by a Time Domain Reflectometry (TDR) equipment. Afterward, plants were kept irrigated until the end of the plant cycle. A simplified schematization of the experiment and timeline can be seen in Fig. 1.

2.2. Leaf gas exchange and chlorophyll a fluorescence

Leaf gas exchange and chlorophyll *a* fluorescence measurements were performed 7 days (7DD) and 20 days after beginning the drought

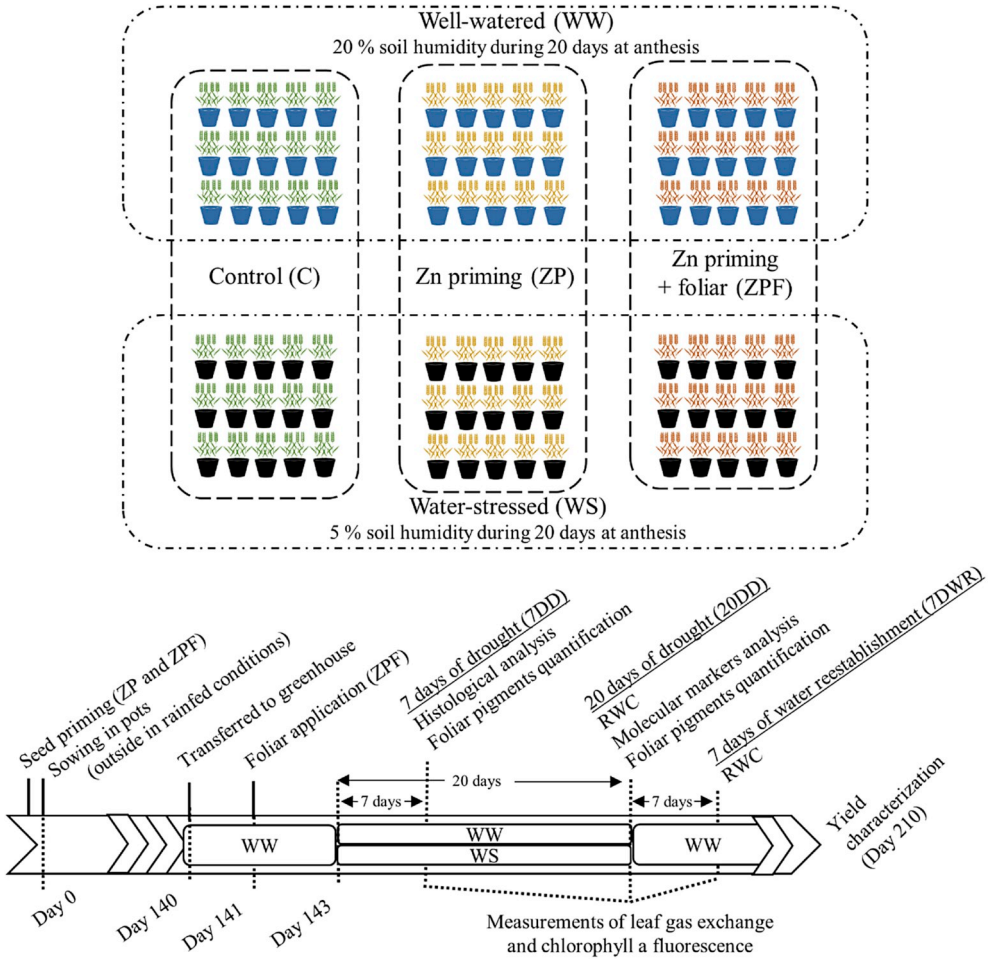

Fig. 1. Simplified schematization and timeline of the experiment.

stress (20DD), and 7 days after water reestablishment (7DWR) (Fig. 1). In plants not subjected to stress, the measurements were performed in the same days. Leaf gas exchange measurements were performed using a portable IRGA (LCpro+, ADC, Hoddesdon, UK), operating in the open mode. Measurements were performed under day's natural irradiance and environmental conditions on sun-exposed leaves. Net photosynthetic rate (A, μmol CO_2 m^{-2} s^{-1}), stomatal conductance for water vapor (g_s, mmol H_2O m^{-2} s^{-1}) and intracellular CO_2 concentration/ambient CO_2 ratio (C_i/C_a) were estimated using the equations developed by von Caemmerer and Farquhar (1981). Intrinsic water use efficiency was calculated as the ratio of A/g_s (μmol mol^{-1}).

Chlorophyll *a* fluorescence variables were measured in vivo with a pulse-amplitude-modulated fluorometer (FMS 2, Hansatech Instruments, Norfolk, UK) on the same leaves and environmental conditions used for gas exchange measurements. Prior to the measurements, a small part of the leaves was dark-adapted for 30 min using dark-adapting leaf-clips. After the dark-adaptation period, the minimal fluorescence (F_o) was measured when all photosystem II (PSII) reaction centers are open, using a low intensity pulsed measuring light source. The maximal fluorescence (F_m) was measured when all PSII reactions centers are closed during a pulse saturating light (0.7 s pulse of 15000 μmol photons m^{-2} s^{-1} of white light). The difference between these two levels (F_m-F_o) was called variable fluorescence (F_v). Maximum quantum efficiency of PSII was calculated as F_v/F_m = (F_m-F_o)/F_m (Krause and Weis, 1991). Following F_v/F_m estimation, after a 20 s exposure to actinic light (1500 μmol m^{-2} s^{-1}), light-adapted steady-state fluorescence yield (F_s) was averaged over 2.5 s, followed by exposure to saturating light (15000 μmol m^{-2} s^{-1}) for 0.7 s to establish F'_m. The sample was then shaded for 5 s with a far-red light source to determine F'_o. Several fluorescence attributes were the calculated (Bilger and Schreiber, 1986; Genty et al., 1989): photochemical quenching (q_P = (F'_m-F_s)/(F'_m-F'_0)), non-photochemical quenching (NPQ = (F_m–F'_m)/F'_m) and efficiency of electron transport as a measure of the quantum effective efficiency of PSII (ϕ_{PSII} = $\Delta F/F'_m$ = (F'_m-F_s)/F'_m). The fraction of light absorbed by the PS II antennae that is dissipated thermally via Δ_{pH} and/or xanthophyll-regulated processes (ϕ_{NPQ}) was calculated as $\phi_{NPQ} = F_s/F'_m - F_s/_{Fm}$ (Hendrickson et al., 2004). The quantum yield of non-regulated energy dissipation, *i.e.,* the sum of the fractions of light absorbed by the PSII antennae that are lost by either constitutive thermal dissipation or via fluorescence was calculated as $\phi_{NO} = F_s/F_m$ (Hendrickson et al., 2004). The apparent electron transport rate was estimated as ETR (μmol $e - m^{-2}$ s^{-1}) = ($\Delta F/F'_m$) x PPFD x 0.5 × 0.84, where PPFD is the photosynthetic photon flux density incident on the leaf, 0.5 is the factor that assumes equal distribution of energy between the two photosystems, and the leaf absorbance used was 0.84, a common value for C_3 plants (Bilger and Schreiber, 1986).

2.3. Leaf structural analysis and water status

Flag leaves were collected 7 days (7DD) and 20 days after beginning the drought stress (20DD), and 7 days after water reestablishment (7DWR). The collected leaves were immediately placed into air-tight containers. Flag leaves collected at 7DD were selected for histological analysis. The mid-section of leaves were prepared by fixation in FAA (formalin-acetic acid-alcohol, 5:5:90 v/v), for 24 h. Leaf sections were

Table 1
LTR, ISSR and PBS primers individually tested in this study.

Type of primer	Primer name	Sequence 5′→3′	Reference
LTR	6149	CTCGCTCGCCCACTACATCAACCGCGTTTATT	Kalendar et al. (1999)
	6150	CTGGTTCGGCCCATGTCTATGTATCCACACATGGTA	
	7286	GGAATTCATAGCATGGATAATAAACGATTATC	
	5′LTR BARE-1	ATCATTGCCTCTAGGGCATAATTC	Saeidi et al. (2008)
	Nikita	CGCATTTGTTCAAGCCTAAACC	Shirasu et al. (2000)
	Sukkula	GATAGGGTCGCATCTTGGGCGTGAC	Bento et al. (2008)
	Sabrina	GCAAGCTTCCGTTTCCGC	
	Tagermina	AGAGGAGGATATCCCAACAT	Queen et al. (2004)
	Thv 19	GCCCAACCGACCAGGTTGTTACAG	
	Tar 1	CTCCCAGTTGACCAACAA	
ISSR	8081	GAGAGAGAGAGAGAGAGAC	Kalendar et al. (1999)
	8082	CTCTCTCTCTCTCTCTCTG	
	8564	CACCACCACCACCACCACCACT	
PBS	*F0100*	TAGGTCGGAACAGGCTCTGATACCA	Wegscheider et al. (2009)
	2222	ACTTGGATGCCGATACCA	Kalendar et al. (2010)
	2224	ATCCTGGCAATGGAACCA	
	2228	CATTGGCTCTTGATACCA	
	2229	CGACCTGTTCTGATACCA	
	2230	TCTAGGCGTCTGATACCA	

dehydrated by immersing them 1 h, in sequentially increasing ethanol concentrations (70%, 80%, 90%, 95%, and 100%). Samples were cleared by placing them in xylene and then embedded in liquid paraffin, using a Leica EG1160 paraffin embedding station. Four μm cross-sections were obtained using a rotary microtome (Leica RM 2135, Germany), placed on slides, and stained with toluidine blue. Cross-sections images were obtained in a microscope Olympus BX41 using a CCD digital camera XC-10 (Olympus America, Inc., New York, USA) and the software CellSens (Olympus Soft Imaging Solutions GmbH, Miinster, Germany). In the midsection of the leaf, thickness of the leaf (LT), mesophyll thickness (MT), lower cuticle (LCT), upper cuticle (UCT), lower epidermis (LET) and, upper epidermis (UET) were measured. In the midrib vascular bundle, the number of metaxylem vessel (MXV) and the total area of the metaxylem vessel (MXVA), protoxylem vessel (PXVA) and phloem tissue (PA) were recorded. All measurements were performed using Digimizer Image Analysis Software (Medcalc, Ostend, Belgium). Flag leaves collected 20DD and 7DWR were examined for the following parameters: fresh weight (FW; g); fresh weight at full turgor (TW; g), measured after immersion of leaf sections in demineralized water for 24 h in the dark at 4 °C; leaf area (LA, cm^2), measured using the WinDias image analysis system (Delta-T Devices Ltd., Cambridge, UK); and dry weight (DW; g), measured after drying in a force-draft oven at 70 °C to a constant weight. Furthermore, to characterize the leaf water status, relative water content (RWC) was calculated as RWC (%) = (FW − DW)/(TW − DW) × 100; the leaf succulence (LS) as LS (g m^{-2}) = (FW-DW)/LA × 1000; and leaf density (LD) as LD (g kg^{-1}) = FW/DW × 1000.

2.4. Photosynthetic pigments quantification

Leave samples from five plants per treatment were collected at 7DD and 20DD. The collected samples were immediately frozen in liquid nitrogen. Later, the leaves were grounded with liquid nitrogen and then stored at −80 °C until use.

Chlorophylls and carotenoids were extracted, as described by Carvalho et al. (2016), from 10 mg of sample in 3 ml acetone in Tris-HCl 100 mM buffer, pH 7.5 (80:20). Absorbance was measured at 470, 537, 647 and 663 nm for carotenoids (Car), anthocyanins, chlorophyll *a* (Chl_a) and chlorophyll *b* (Chl_b), respectively. Pigment concentrations were calculated using the equations described by Sims and Gamon (2002): Chl_a (μmol ml^{-1}) = 0.01373 × A_{663} - 0.000897 × A_{537} - 0.003046 × A_{647}; Chl_b (μmol ml^{-1}) = 0.02405 × A_{647} - 0.004305 × A_{537} - 0.005507 × A_{663}; $Chl_{(a+b)}$ (μmol ml^{-1}) = Chl_a + Chl_b, Car (μmol ml^{-1}) = (A_{470} - 17.1 × $Chl_{(a+b)}$ - 9.479 × anthocyanins)/119.26; anthocyanins (μmol ml^{-1}) = 0.08173 × A_{537} - 0.00697 × A_{647} - 0.002228 × A_{663}. $Chl_{(a+b)}$. Results for $Chl_{(a+b)}$ and Car were converted to mg g^{-1} of FW considering the molecular weight of Chl_a = 893.5 g mol^{-1}, Chl_b = 904.5 g mol^{-1}, and Car = 550 g mol^{-1}.

2.5. Genomic stability

Leaves collected at the end of the drought period (20DD) were immediately frozen in liquid nitrogen and maintained at −80 °C. Genomic DNA extraction was performed using a CTAB-based method (Doyle and Doyle, 1987). The DNA samples were quantified in the spectrophotometer Nanodrop ND-1000 (Thermo Scientific) and their integrity were evaluated after electrophoresis on a 0.8% agarose gel. Working solutions with 25 ng μL^{-1} of concentration were prepared. Subsequently, DNA samples were used for the amplification of retrotransposon-based (IRAP, REMAP and iPBS) and gene-target (SCoT and CDDP) molecular markers.

2.5.1. Retrotransposon-based molecular markers

Different LTR, SSR and PBS primers that were designed and/or previously used by other authors to amplify IRAP, REMAP, ISSR and iPBS markers in wheat and other cereals were tested (Table 1). The LTR and SSR primers, as well as the individual PBS primers that showed successful amplification were combined among them for the production of REMAP and additional iPBS markers, respectively (Table 2). The PCR mixture, the amplification and electrophoresis conditions used for the production of retrotransposon-based markers were those described in Cabo et al. (2014a).

2.5.2. Gene-target molecular markers

The 36 SCoT primers previously developed by Collard and Mackill (2009b) were tested. For the amplification of CDDP markers, we tested

Table 2
Selected combinations of primers for the amplification of IRAP, REMAP, ISSR and iPBS markers in this study and which also were successful in previous studies performed in cereals.

Marker	Primers combination	Reference
IRAP	*5'LTR BARE-1 + Sukkula*	Carvalho et al. (2010); Carvalho et al. (2012)
	6149 + Sukkula	
	6150 + Sukkula	
	Nikita + Sukkula	
	Sukkula	Bento et al. (2008); Carvalho et al. (2010); Carvalho et al. (2012); Cabo et al. (2014a)
REMAP	*7286 + 8081*	Carvalho et al. (2010); Carvalho et al. (2012)
	Nikita + 8081	
	Sukkula + 8081	Carvalho et al. (2010); Carvalho et al. (2012); Cabo et al. (2014a)
ISSR	*8081*	Kalendar et al. (1999); Carvalho et al. (2010); Carvalho et al. (2012); Cabo et al. (2014a)
iPBS	*F0100*	Wegscheider et al. (2009); Cabo et al. (2014a)

Table 3
Primers tested in this work for CDDPs amplification: name of the stress-responsive genes, respective GenBank accessions, sequences and references.

Gene	GenBank accession	Sequence 5'→3'	Reference
TaWRKY1	KT285206	F: ATATGGCGGCACTTGTCACT R: CAGAGGAATGGCGTCAAAAT	He et al. (2016)
TaWRKY33	KT285207	F: GAGGTTGCGGTTCTTGAGTC R: AGGTTCCGACGGATCATCT	
TaWRKY44	KR827395	F: GCCCCCCTTCGCTCTTCTC R: CAGCACACCAGAAATGGGCTAAT	Wang et al. (2015)
TaPIMP1 (Myb gene)	EF587267	MQC-F: ACTCGCGTACGTCTTCCTGA MQC-R: GCGCTCTAGTTAAGTTCATCGTC	Liu et al. (2011)

the forward and reverse primers of the water stress-responsive genes (Table 3) previously isolated and characterized by other authors (He et al., 2016; Liu et al., 2011; Wang et al., 2015). Additionally, we designed specific primers for the sequences of genes *TaWRKY1* and *TaWRKY33*, publicly available in GenBank (Table 3), using the software Primer3 (v. 0.4.0) (Koressaar and Remm, 2007; Untergasser et al., 2012) and the following criteria: primer length of 18–20 base pair (bp), GC content of 45–60%, and melting temperature (Tm) of 60 °C. The PCR mixture and amplification conditions of the SCoT markers were the same reported by Cabo et al. (2014b). For CDDPs amplification, we used the PCR mixture, amplification and electrophoresis conditions described by Collard and Mackill (2009a).

2.5.3. Scoring and analysis

The molecular weight marker Gene Ruler 100 bp Plus DNA Ladder (Thermo Scientific) was loaded on each agarose gel. The bands were analysed for their presence (1) or absence (0). Bands with the same molecular weight produced by the same primer were considered the same locus. ISSRs and IRAPs are amplified with a single SSR and LTR primer, respectively, REMAP bands with an equal molecular weight to ISSRs and/or IRAPs produced with the same primer were discarded from the REMAP matrix, in order to ensure the effective analysis of REMAP markers.

To assess if water availability (W) or treatment (T) affected genomic stability, well-watered plants without any Zn treatments (WW × C) were considered as control. Polymorphism verified in the remaining treatments (WW × ZP, WW × ZPF, WS × C, WS × ZP, WS × ZPF) included the disappearance of 'normal' bands or appearance of new bands. In the present context, 'normal' bands denotates monomorphic band in control (WW × C). Genomic Template Stability (GTS) was calculated as follows: GTS (%) = 100-(100 × *a*/*n*), where a is the polymorphic (disappearance or appearance) of bands in each treatment and *n* is the total number of monomorphic bands considered in control (WW × C).

GenAlEx v6.51b2 (Peakall and Smouse, 2006) was used to create a Pairwise Matrix of Binary Genetic Distance among plants from different treatments followed by Principal Coordinates Analysis (PCoA). Excel 3D Scatter Plot' v2.1 (http://www.doka.ch/Excel3Dscatterplot.htm) was used to create a 3-dimensional PCoA (3D-PCoA), showing the three main axes (x, y, and z), based on the results of the GenAlEx v6.51b2. Retrotransposon-based (IRAP, REMAP and iPBS) and gene-target (SCoT and CDDP) molecular markers were analysed separately.

2.6. Yield assessment

At the end of the experiment (Day 210), five pots (a total 20 plant) per treatment were characterized for above ground plant biomass, as well as grain number and weight. Harvest index (HI) was calculated as HI (%) = [grain weight]/[plant biomass] × 100. Extrapolated 1000 grain weight was calculated as [grain weight]/[number of grain] × 1000.

2.7. Statistical analysis

A two-way Analysis of Variance (2 way-ANOVA) and Tukey post-hoc test were performed to determine the effect of the water availability (W), treatment (T), and the interaction of both factors (W × T) on the investigated morphological, histological, physiological and foliar pigment parameters. These analyses were performed with the IBM SPSS Statistics V23 (IBM Corporation, Armonk, USA). Most of the results are presented as mean values. For statistical analysis, arcsine transformation was performed in percentage data, namely for RWC (original values are shown).

3. Results

3.1. Leaf gas exchange and chlorophyll a fluorescence

Leaf gas exchange measurements were performed 7 days (7DD) and 20 days after beginning the drought stress (20DD), and 7 days after water reestablishment (7DWR) (Fig. 2). A drought-induced decline in net photosynthetic rate (A) was recorded (Fig. 2a). The lowest mean value was recorded at 20DD in control plants (WS × C). After rewatering (7DWR), net photosynthesis of plants treated with Zn (ZP and ZPF) recovered to values similar to well-watered plants (WW). Conversely, WS × C presented only a small increase in A (Fig. 2a). Stomatal conductance for water vapor (g_s) showed similar tendency as A across all dates (Fig. 2b). Plants subjected to drought presented higher intrinsic water use efficiency (A/g_s) during the drought induction period (7DD and 20DD) (Fig. 2c). After rewatering (7DWR) A/g_s was not affected ($p > 0.05$) by W, T or W × T (Fig. 2c). The intracellular CO_2/ambient CO_2 ratio (C_i/C_a), at 7DD, was lower in plants subjected to drought, when compared with non-stressed plants (Fig. 2d). At the same date, control plants (C) presented higher C_i/C_a when compared with zinc-treated plants (ZP and ZPF). At the end of the drought period (20DD), C_i/C_a values were affected ($p = 0.003$) by W × T (Fig. 2d) with the lowest value recorded in WS × ZPF and the highest in WW × ZPF

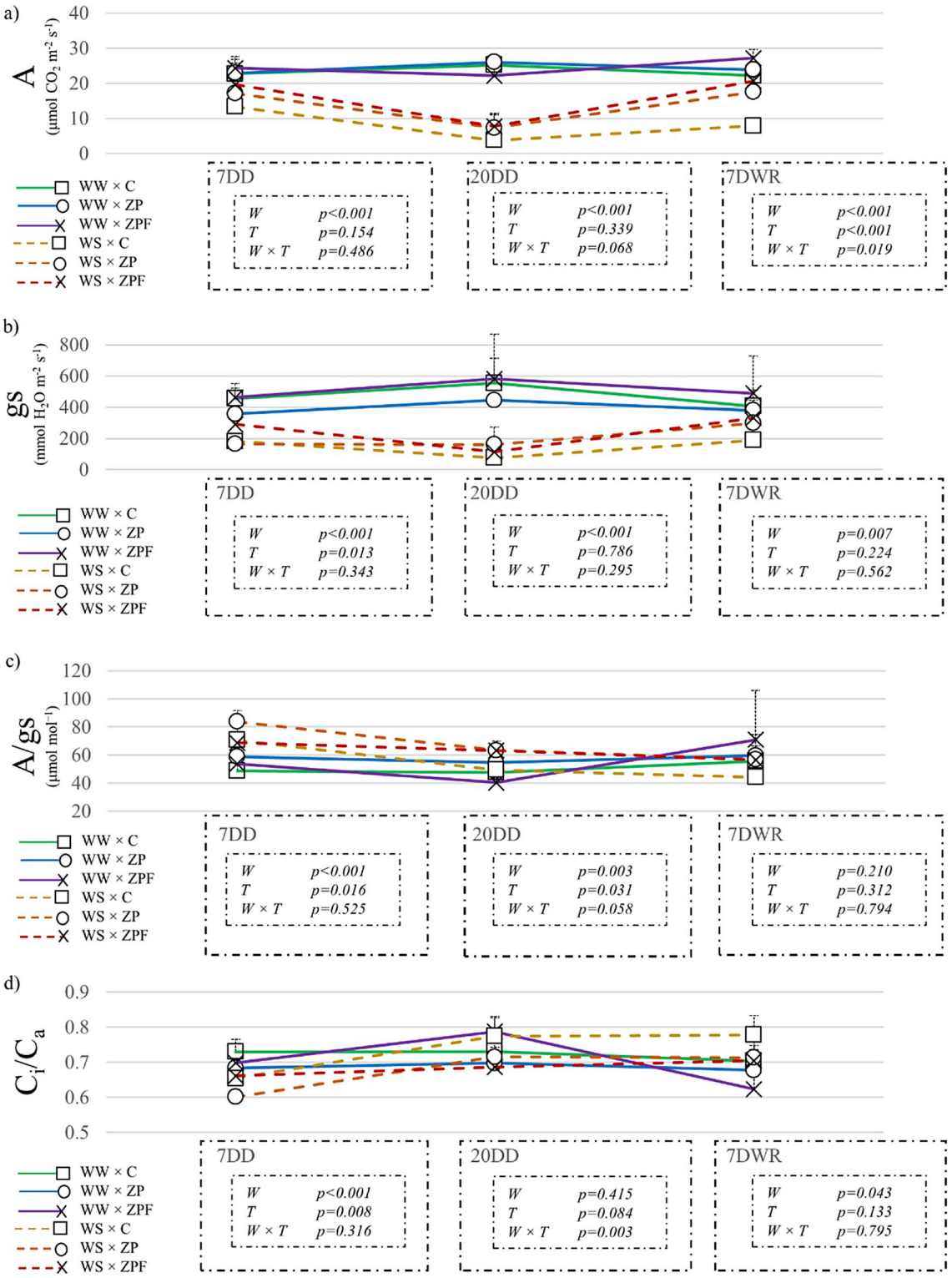

Fig. 2. Variations in net photosynthetic rate (A, a), stomatal conductance for water vapor (g_s, b), intrinsic water use efficiency (A/g_s, c) and intracellular/ambient CO_2 concentration ratio (C_i/C_a, d) during drought (7DD and 20DD) and recovery (7DWR). Measurements performed in leaves of control (C), zinc primed (ZP) and zinc primed plus foliar application (ZPF) of well-watered (WW) and water-stressed (WS) wheat plants at anthesis. Results of two-way ANOVA are shown. Different letters (a,b,c) per date indicate statistical significant differences ($p < 0.05$) showed by the Tukey test.

(Fig. 2d). At 7DWR, C_i/C_a mean values were higher in plants which had been subjected to drought (Fig. 2d).

The maximum (F_v/F_m) and actual quantum efficiency of photosystem II (ϕ_{PSII}), the photochemical fluorescence quenching (q_P), the capture and the efficiency of excitation energy by open PSII reaction centers (F'_v/F'_m) and the electron transport rate (ETR) decreased in water-stressed plants (WS), at all dates (Table 4). The highest difference between WW and WS values of ϕ_{PSII}, q_P, F'_v/F'_m and ETR were noted at the end of the drought period (20DD). After rewatering (7DW), plants subject to drought and treated with Zn (WS × ZP and WS × ZPF)

Table 4
Mean values of maximum (F_v/F_m) and actual (ϕ_{PSII}) quantum efficiency of photosystem II, photochemical fluorescence quenching (q_P), capture efficiency of excitation energy by open PSII reaction centers (F'_v/F'_m), electron transport rate (ETR) and non-photochemical quenching (NPQ) of wheat plants subjected to different water availability (W), Zn treatments (T) and interaction of W × T. Measurements performed 7 (7DD) and 20 days (20DD) after the beginning of drought stress and 7 days after water reestablishment (7DRW). p-values are shown for W, T and W × T. Mean values with different letters (a,b,c) per column indicate statistical significant differences ($p < 0.05$) showed by the Tukey test.

	7DD						20DD						7DWR					
	F_v/F_m	ϕ_{PSII}	q_P	F'_v/F'_m	ETR (μmol m^{-2} s^{-1})	NPQ	F_v/F_m	ϕ_{PSII}	q_P	F'_v/F'_m	ETR (μmol m^{-2} s^{-1})	NPQ	F_v/F_m	ϕ_{PSII}	q_P	F'_v/F'_m	ETR (μmol m^{-2} s^{-1})	NPQ
Water availability (W)																		
Well-watered (WW)	0.884	0.594	0.789	0.763	212.0	1.41	0.898	0.596	0.772	0.773	234.1	1.563	0.884	0.631	0.819	0.770	247.5	1.03
Water-stressed (WS)	0.874	0.515	0.716	0.729	183.8	1.36	0.877	0.327	0.589	0.525	128.3	0.725	0.851	0.458	0.679	0.676	177.1	1.93
Treatment (T)																		
Control (C)	0.877	0.583	0.791	0.748	208.0	1.74 a	0.882	0.473	0.674	0.647	185.9	0.862 b	0.852	0.522	0.739	0.680	205.0	2.07
Zn priming (ZP)	0.877	0.539	0.730	0.756	192.4	1.21 b	0.890	0.434	0.696	0.611	170.3	1.116 a,b	0.870	0.560	0.762	0.735	219.6	1.36
Zn priming + Foliar application (ZPF)	0.883	0.542	0.737	0.735	193.5	1.21 b	0.891	0.478	0.673	0.690	187.5	1.455 a	0.880	0.552	0.747	0.755	212.4	1.02
W × T																		
WW × C	0.882	0.614	0.806	0.762	219.0	1.52	0.896	0.641	0.778	0.820	251.9	1.537	0.892	0.642	0.854	0.742	251.9	1.11
WW × ZP	0.887	0.618	0.827	0.778	220.5	1.38	0.903	0.560	0.788	0.716	219.7	1.513	0.869	0.626	0.817	0.775	245.7	1.11
WW × ZPF	0.883	0.551	0.735	0.749	196.6	1.33	0.895	0.587	0.751	0.783	230.6	1.639	0.891	0.624	0.787	0.792	244.8	0.87
WS × C	0.872	0.552	0.775	0.733	196.9	1.95	0.868	0.305	0.569	0.474	119.9	0.186	0.812	0.402	0.624	0.617	158.0	3.02
WS × ZP	0.867	0.460	0.633	0.734	164.2	1.04	0.877	0.308	0.603	0.505	120.8	0.718	0.871	0.493	0.706	0.694	193.5	1.61
WS × ZPF	0.882	0.533	0.739	0.721	190.4	1.09	0.886	0.368	0.595	0.596	144.3	1.271	0.869	0.479	0.706	0.718	179.9	1.17
p values																		
W	0.051	0.001	0.002	0.037	0.001	0.807	< 0.001	< 0.001	< 0.001	< 0.001	< 0.001	< 0.001	0.047	< 0.001	< 0.001	0.042	< 0.001	0.003
T	0.640	0.198	0.057	0.553	0.198	0.044	0.258	0.229	0.794	0.094	0.229	0.007	0.347	0.673	0.773	0.328	0.673	0.113
W × T	0.325	0.050	0.002	0.895	0.050	0.208	0.187	0.110	0.822	0.063	0.110	0.025	0.123	0.427	0.084	0.872	0.427	0.158

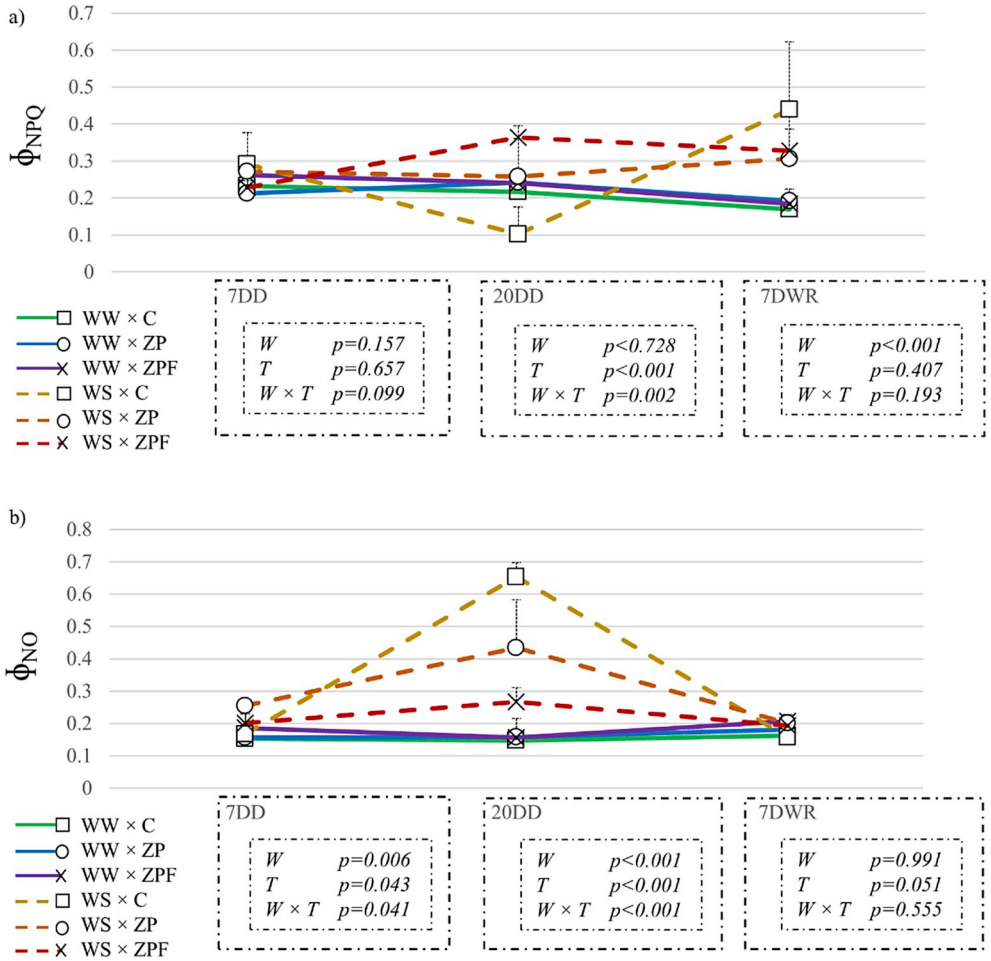

Fig. 3. Variation in the quantum yield of regulated (ϕ_{NPQ}, a) and non-regulated energy dissipation (ϕ_{NO}, b) during drought (7DD and 20DD) and recovery (7DWR). Measurements performed in leaves of control (C), zinc primed (ZP) and zinc primed plus foliar application (ZPF) of well-watered (WW) and water-stressed (WS) wheat plants at anthesis. Results of two-way ANOVA are shown. Different letters (a,b,c) per date indicate statistical significant differences ($p < 0.05$) showed by the Tukey test.

presented higher ϕ_{PSII}, q_P, F'_v/F'_m and ETR than WS × C (Table 4). Meanwhile, non-photochemical quenching (NPQ) was significantly higher ($p = 0.044$) in control plants (C), at 7DD, than ZP and ZPF. At the end of the drought period (20DD), the lowest NPQ mean values were recorded at WS × C with a mean of 0.186. Zn treated plants, WS × ZP, and WS × ZPF, presented mean values of 0.718 and 1.271, respectively. At the same date, WW plants presented a mean value of 1.563. After rewatering (7DWR), WW plants presented a lower NPQ value of 1.03, while WS × C presented 3.02, and WS × ZP and WS × ZPF presented values of 1.61 and 1.17, respectively (Table 4).

The results for the fraction of light absorbed by the PSII antennae that are dissipated thermally via ΔpH and/or xanthophyll-regulated processes (ϕ_{NPQ}) are present in Fig. 3a. Overall well-watered plants (WW), independently of the treatment, showed similar ϕ_{NPQ} values across the three dates, ranging from a mean of 0.170–0.262. At the end of the drought period (20DD), the lowest ϕ_{NPQ} mean values were registered at WS × C with 0.103 (Fig. 3b). At this date, WS × ZP and WS × ZPF presented an over 2- and 3-fold increase in ϕ_{NPQ} mean values when compared with WS × C (Fig. 3b). After rewatering, WS presented significantly ($p < 0.001$) higher ϕ_{NPQ} mean values of 0.358 when compares with WW, with 0.183 (Fig. 3a). On the other hand, the sum of the fractions of light absorbed by the PSII antennae that is lost by either constitutive thermal dissipation or via fluorescence (ϕ_{NO}) was affected ($p < 0.05$) by treatment (T), water availability (W) and the interaction of W × T, during the drought induction period (Fig. 3b). Well-watered plants (WW), independently of the treatment, showed similar ϕ_{NO} values across the three dates, with an overall mean of 0.168. The highest ϕ_{NO} values were recorded at the end of the drought period in not treated plants (WS × C). Among the plants subjected to drought, plants where Zn was foliar applied presented the lowest ϕ_{NO} values at 20DD. After rewatering plants subjected to drought presented similar ϕ_{NO} values of non-stressed plants.

3.2. Leaf structural analysis and water status

Leaf structure analysis was performed in flag leaves collected at 7DD (Table 5). Leaf thickness (LT) significantly increased in plants subjected to drought stress ($p = 0.043$) and in plants where Zn was applied in the leaves (ZPF) ($p = 0.005$). Mesophyll tissue (MT) and upper epidermis tissue (UET) also significantly ($p < 0.05$) increased in ZPF (Table 5). Both the lower (LCT) and upper cuticle tissue (UCT) increased in plants subjected to drought ($p < 0.003$). The treatment ZPF caused a decrease in UCT ($p < 0.001$) to a mean of 1.81 μm when compared with 2.52 μm in C and 2.31 μm in ZP (Table 5). The number of metaxylem vessels (MXV) significantly increased ($p = 0.027$) when drought was applied from 2.00 in WW to a mean of 2.33 in WS (Table 5). Conversely, the total metaxylem (MXVA) and protoxylem vessel area (PXVA) was not affected ($p > 0.1$) by W or T (Table 5). Total phloem tissue area (PA) increased ($p = 0.047$) from a mean of 1187.6 and 1193.5 μm^2 in C and ZP, respectively, to 1409.1 μm^2 in ZPF (Table 5).

Table 5
Mean values of leaf thickness (LT), mesophyll tissue (MT), lower cuticle tissue (LCT), upper cuticle tissue (UCT), lower epidermis tissue (LET), upper epidermis tissue (UET), number of metaxylem vessel (MXV), total metaxylem vessel area (MXVA), total protoxylem vessel area (PXVA) and total phloem tissue area (PA) of wheat plants subjected to different water availability (W), Zn treatments (T) and interaction of W × T. p-values are shown for W, T and W × T. Mean values with different letters (a,b,c) per column indicate statistical significant differences ($p < 0.05$) showed by the Tukey test.

	LT (μm)	MT (μm)	LCT (μm)	UCT (μm)	LET (μm)	UET (μm)	Number of MXV	Total MXVA (μm^2)	Total PXVA (μm^2)	Total PA (μm^2)
Water availability (W)										
Well-watered (WW)	165.5	143.4	3.02	2.02	10.9	12.5	2.00	1058.3	236.7	1225.9
Water-stressed (WS)	179.9	149.4	3.77	2.40	11.5	13.0	2.33	1222.8	264.5	1300.9
Treatment (T)										
Control (C)	162.7 b	143.3 b	3.46	2.52 a	11.3	12.6 a,b	2.10	1069.2	220.4	1187.6
Zn priming (ZP)	165.0 b	140.6 b	3.31	2.32 a	10.6	11.6 b	2.40	1104.3	248.4	1193.5
Zn priming + Foliar application (ZPF)	190.4 a	155.5 a	3.42	1.81 b	11.8	14.0 a	2.00	1248.2	283.1	1409.1
W × T										
WW × C	154.5	143.1	3.36	2.37	10.6	11.7	2.00	1021.6	234.6	1187.7
WW × ZP	152.9	133.5	2.90	2.09	10.1	11.1	2.00	867.1	172.9	1103.4
WW × ZPF	189	153.7	2.79	1.61	12.0	14.6	2.00	1286.1	302.6	1386.5
WS × C	170.9	143.4	3.55	2.66	12.0	13.4	2.20	1116.8	206.2	1187.5
WS × ZP	177.1	147.6	3.71	2.54	11.0	12.1	2.80	1341.4	323.8	1283.6
WS × ZPF	191.7	157.2	4.05	2.00	11.6	13.4	2.00	1210.2	263.6	1431.6
p values										
W	0.043	0.157	< 0.001	0.003	0.219	0.352	0.027	0.107	0.347	0.356
T	0.005	0.014	0.697	< 0.001	0.152	0.001	0.075	0.306	0.226	0.047
W × T	0.407	0.369	0.016	0.879	0.337	0.066	0.075	0.085	0.024	0.643

Table 6
Mean values of leaf relative water content (RWC), leaf succulence (LS), and leaf density (LD) of wheat plants subjected to different water availability (W), Zn treatments (T) and interaction of W × T. Samples collected 20 days after the beginning of drought stress (20DD) and 7 days after water reestablishment (7DWR). p-values are shown for W, T and W × T. Mean values with different letters (a,b,c) per column indicate statistical significant differences ($p < 0.05$) showed by the Tukey test.

	20DD			7DWR		
	RWC (%)	LS ($g\ m^{-2}$)	LD ($g\ Kg^{-1}$)	RWC (%)	LS ($g\ m^{-2}$)	LD ($g\ Kg^{-1}$)
Water availability (W)						
Well-watered (WW)	87.5	12.19	293.9	95.3	12.8	290.8
Water-stressed (WS)	63.3	8.87	372.3	93.2	12.3	291.5
Treatment (T)						
Control (C)	75.1	10.53	345.7	94.1	11.3 a	302.8
Zn priming (ZP)	76.2	10.17	318.9	94.9	13.4 b	280.7
Zn priming + Foliar application (ZPF)	75.0	10.89	334.9	93.9	13.1 b	290.1
W × T						
WW × C	86.4	12.00	297.7	95.7	11.5	299.7
WW × ZP	89.7	12.23	291.1	95.4	13.5	288.2
WW × ZPF	86.5	12.33	293.0	94.8	13.4	284.6
WS × C	63.8	9.05	393.7	92.4	11.0	305.9
WS × ZP	62.7	8.10	346.6	94.3	13.2	273.1
WS × ZPF	63.4	9.45	376.7	92.9	12.8	295.6
p values						
W	< 0.001	< 0.001	< 0.001	0.022	0.312	0.924
T	0.975	0.683	0.362	0.593	0.003	0.056
W × T	0.899	0.687	0.543	0.577	0.986	0.259

At the end of the drought period (20DD), plants subjected to drought (WS) showed a significantly ($p < 0.001$) lower leaf relative water content (RWC) of 63.3%, when compared with RWC values of 87.5% of control plants (Table 6). After rewatering (7DWR), plants that endured drought still presented a lower RWC value (Table 6). Leaf succulence (LS) values were significantly lower ($p < 0.001$) in drought-stressed plants at 20DD (Table 6). Contrastingly, at 7WR, LS was affected by treatment (T) ($p = 0.003$), showing higher values in Zn treated plants (ZP and ZPF) (Table 6). WS plants presented higher leaf density (LD) at 20DD. At 7DWR, LD was not affected ($p > 0.05$) by W, T or W × T (Table 6).

3.3. Foliar pigments quantification

Total chlorophylls ($Chl_{(a+b)}$), chlorophyll *a/b* ratio (Chl_a/Chl_b), total carotenoids (Car) and total chlorophylls/total carotenoids ratio ($Chl_{(a+b)}$/Car) were characterized in flag leaves collected at collected 7 (7DD) and days (20DD) after the beginning of drought stress (Table 7). $Chl_{(a+b)}$ and Car were not affected ($p > 0.1$) by W, T or W × T, at neither 7DD or 20DD (Table 7). Drought stress, at 7DD, significantly decreased ($p < 0.001$) the Chl_a/Chl_b mean value of 3.20 in WW to 2.72 in WS (Table 7). At 20DD, Chl_a/Chl_b was not affected ($p > 0.05$) by either W, T or W × T (Table 7). $Chl_{(a+b)}$/Car was not affected

Table 7
Mean values of total chlorophylls ($Chl_{(a+b)}$), chlorophyll *a*/b ratio (Chl_a/Chl_b), total carotenoids (Car) and total chlorophylls/total carotenoids ratio ($Chl_{(a+b)}$/Car) of leaves of wheat plants subjected to different water availability (W), Zn treatments (T) and interaction of W × T. Samples collected 7 days (7DD) and 20 days (20DD) after the beginning of drought stress. p-values are shown for W, T and W × T. Mean values with different letters (a,b,c) per column indicate statistical significant differences ($p < 0.05$) showed by the Tukey test.

	7DD				20DD			
	$Chl_{(a+b)}$ (mg g^{-1} of FW)	Chl_a/Chl_b	Car (mg g^{-1} of FW)	$Chl_{(a+b)}$/Car	$Chl_{(a+b)}$ (mg g^{-1} of FW)	Chl_a/Chl_b	Car (mg g^{-1} of FW)	$Chl_{(a+b)}$/Car
Water availability (W)								
Well-watered (WW)	1.36	3.20	0.275	4.88	1.43	3.03	0.269	5.35
Water-stressed (WS)	1.22	2.72	0.246	4.89	1.24	2.94	0.287	4.40
Treatment (T)								
Control (C)	1.28	2.99	0.261	4.82	1.41	3.04	0.295	4.95
Zn priming (ZP)	1.45	2.94	0.298	4.89	1.12	2.97	0.250	4.64
Zn priming + Foliar application (ZPF)	1.14	2.94	0.224	4.96	1.49	2.97	0.290	5.03
W × T								
WW × C	1.45	3.07	0.285	5.09	1.32	3.02	0.241	5.51
WW × ZP	1.46	3.01	0.296	4.94	1.02	3.05	0.218	4.97
WW × ZPF	1.16	3.51	0.244	4.62	1.94	3.03	0.348	5.56
WS × C	1.10	2.91	0.236	4.55	1.49	3.05	0.348	4.39
WS × ZP	1.44	2.87	0.299	4.83	1.21	2.88	0.281	4.31
WS × ZPF	1.11	2.37	0.203	5.29	1.03	2.90	0.231	4.49
p values								
W	0.317	< 0.001	0.249	0.981	0.287	0.399	0.648	< 0.001
T	0.184	0.894	0.068	0.738	0.193	0.792	0.611	0.318
W × T	0.555	< 0.001	0.657	0.008	0.017	0.681	0.052	0.636

($p > 0.1$) by T or W, at 7DD, and mean values ranged between 4.55 and 5.29 (Table 7). At 20DD, $Chl_{(a+b)}$/Car significantly decreased ($p < 0.001$) from a mean value of 5.35 in WW to 4.40 in WS (Table 7).

3.4. Genomic stability

All selected combinations of primers LTR, SSR and PBS (Table 2) produced polymorphic patterns among the tested plants. Five out of the 36 SCoT primers - specifically SCOT 1, SCOT 2, SCOT 4, SCOT 7 and SCOT 11 - showed successful amplification and produced polymorphic patterns among the tested plants. Among the tested CDDP primers (Table 3), all with the exception of TaWRKY33-F showed successful amplification and produced polymorphic patterns. Detailed tables, for all primers, showing the disappearance of 'normal' bands or appearance of new bands of the several treatments (WW × ZP, WW × ZPF, WS × C, WS × ZP, WS × ZPF) is available in supplementary material (Table S1 and Table S2).

Well-watered plants without any Zn treatments (WW × C) were considered as a control for Genomic Template Stability (GTS). GTS, assessed by the retrotransposon-based molecular markers, ranged between 56.7 and 94.0% among the considered treatments (WW × ZP, WW × ZPF, WS × C, WS × ZP, WS × ZPF) (Fig. 4). GTS, assessed by the gene-target molecular markers, ranged between 68.3 and 79.4%. The highest GTS value was verified in WW × ZP by both molecular marker systems (Fig. 4). The lowest GTS value was verified in WW × ZPF by the retrotransposon-based molecular markers (Fig. 4).

The genomic variation for each water availability × treatment combination (W × T) is represented in a 3-dimensional Principal Coordinates Analysis (3D-PCoA) (Fig. 5). The results are presented separately by retrotransposon-based (Fig. 5a) and gene-target (Fig. 5b) molecular markers. The combination of the 3 main axes (x, y, and z) explains 100.00% of the variability detected by the retrotransposon-based molecular markers (Fig. 5a). Considering x- and y-axis, which combined explains 89.92% of the detected genetic variability, plants subjected to drought (WS) are all clustered in the 2nd quadrant. Plants not subjected to drought and where Zn was applied in the leaves (WW × ZPF) are represented in the 1st quadrant, while the remaining

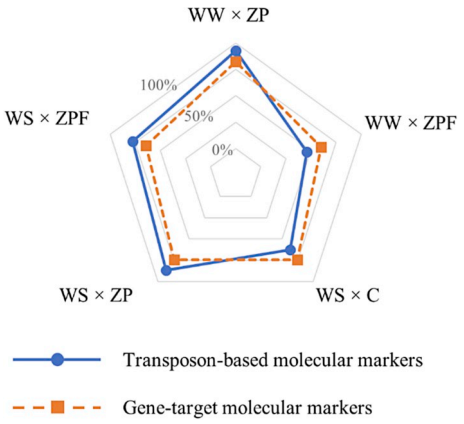

Fig. 4. Genomic template stability (GTS) assessed by retrotransposon-based and gene-target molecular markers of well-watered (WW) treated with zinc priming (ZP) and zinc priming plus foliar application (ZPF), and water-stressed (WS, 20DD) of control (C), zinc primed (ZP) and zinc primed plus foliar application (ZPF) wheat plants.

treatments, WW × C and WW × ZP are in the 3rd quadrant. The z-axis explains 10.8% of detected diversity and separates the WS × ZPF from all remaining combinations. Likewise, the combination of the 3 main axes (x, y, and z) explains 92.5% of the variability detected by the gene-target molecular markers (Fig. 5b). The x- and y-axis explains 82.82% of the detected genetic variability, clustered all WS plants in the 1st and 2nd quadrant and WW in the 3rd and 4th quadrant. The z-axis explains 9.68% separates WS × ZPF and WW × ZP from the remaining.

3.5. Yield assessment

The above ground plants biomass, the grain number and weight, harvest index (HI) and the extrapolated weight of 1000 grain are present in Table 8. Drought significantly decreased all of these variables ($p < 0.05$) (Table 8). The number of grains decreased over 60% in plants subjected to drought while 1000 grain weight decreased *c.a.* 12%

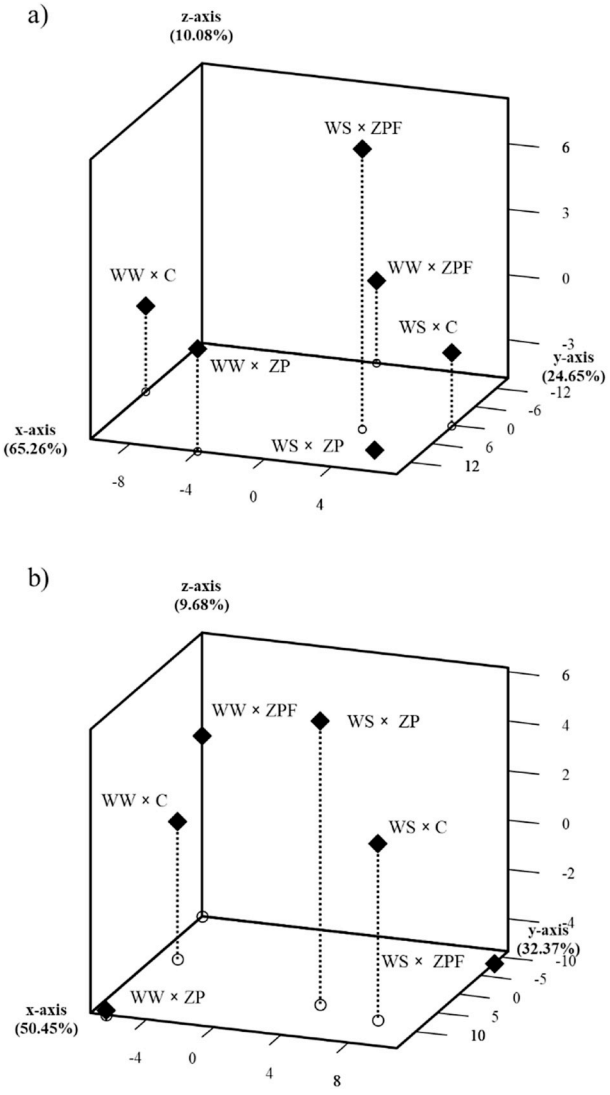

Fig. 5. 3-dimensional Principal Coordinates Analysis (3D-PCoA) of the genetic variation based on transposon-based (a) and gene-target molecular markers (b) performed in leaves of control (C), zinc primed (ZP) and zinc primed plus foliar application (ZPF) of and water-stressed (WS, 20DD) wheat plants at anthesis.

(Table 8). Contrastingly, none of these variables were affected ($p > 0.05$) by Zn treatment (T) or by the interaction W × T (Table 8).

4. Discussion

4.1. Physiological effects of drought and rewatering

Reduction of photosynthesis is one of the major consequences of drought in plants. This decrease may be due to stomatal or non-stomata limitations (Farooq et al., 2009). Stomatal closure is usually considered the determining factor in the reduction of CO_2 assimilation and photosynthesis reduction during drought (Lu and Zhang, 1999; Farooq et al., 2009; Abid et al., 2016). Nonetheless, non-stomatal limitations may also occur at moderate and severe drought events (Brito et al., 2018). In our study, stomatal limitations were observed with proportional decrease of A and g_s during the initial period of drought (Fig. 2), although perturbations on the primary photochemistry of PSII were also observed, as evidenced by the decrease of ϕ_{PSII}, capture efficiency of excitation energy by open PSII reaction centers (F'_v/F'_m) and electron transport rate (ETR) (Table 4). Moreover, at the peak of drought stress (20DD), apart the exacerbation of stomatal and photochemical effects induced by water stress, the biochemical component of photosynthesis was also severely inhibited, judging by changes of g_s, A/g_s and C_i/C_a ratio. In the present study, at the end of the drought period, we recorded a mean RWC value of 63.8% in WS plants, confirming a higher level of drought stress. Indeed, it was reported that with RWC values below 65% the stomata are almost or fully closed (Lawlor and Cornic, 2002; Brodribb and Holbrook, 2003). Under such severe drought stress (RWC < 75), photosynthesis is not only constrained by stomatal limitations, but also by a reduction of the maximum quantum efficiency of photosystem II and decreasing activities of CO_2 assimilating enzymes (Lawlor and Cornic, 2002; Abid et al., 2016). As such, the significant perturbations in chlorophyll *a* fluorescence variables in plants subjected to drought at 20DD (Table 4) is not unexpected. Furthermore, accelerated leaf senescence associated with a decrease in chlorophyll content could be predictable (Farooq et al., 2014; Ahmad et al., 2018). However, we did not observe any significant variation in chlorophyll and carotenoid concentrations in plants subjected to drought (Table 7). Others have also reported a maintenance or even increase of chlorophyll content during drought (Simova-Stoilova et al., 2009; Fahad et al., 2017).

The increase in leaf thickness (LT) under drought stress can allow a higher water use efficiency (Abid et al., 2016). At 7DD we observed an increase in LT in drought-stressed plants (Table 5) coupled with an increase in intrinsic water use efficiency (A/g_s) (Fig. 2). Such adaptations may also enhance the plant's capability to overcome the photoinhibition under drought stress (Izanloo et al., 2008; Abid et al., 2016). Notwithstanding, severely stressed plants may present decreases in MT and consequently of LT due to lack of water (El-Afry et al., 2012). At the end of the drought period (20DD), the decrease in LT is suggested due to the decrease in RWC and leaf succulence (LS) and increase in leaf density (LD) (Table 5).

During stress conditions, the plants are not capable of using a significant part of the absorbed light energy though photosynthesis, or even photorespiration and alternative electron routes (Lawlor and Cornic, 2002; Urban et al., 2017). Indeed, a decrease in que photochemical quenching (q_p) in WS plants during drought was observed (Table 4). The main mechanism by which plants transfer the excess light energy away from photosynthetic electron transport toward heat production is energy-dependent quenching, which depends in part on the xanthophyll cycle (Urban et al., 2017). Correspondingly, an increase in non-photochemical quenching (NPQ) was observed at 7DD in WS × C, when compared with WW × C (Table 4). Surprisingly, at the end of the drought stress a massive decrease in NPQ in WS × C was observed (Table 4). This decrease can be explained observing the quantum yield of light-induced (Δ_{pH}- and zeaxanthin-dependent) non-photochemical fluorescence quenching (ϕ_{NPQ}) and the quantum yield of non-regulated heat dissipation and fluorescence emission (ϕ_{NO}) (Fig. 3). At the end of the drought period, WS × C plants may not be able to safely regulate the dissipation of excess energy, which contributes to a decrease in NPQ. Nonetheless the energy dissipation was achieved by non-regulated mechanisms (ϕ_{NO}). This hypothesis is supported by the results presented in Fig. 3, where a decrease in ϕ_{NPQ} was accompanied with an increase in ϕ_{NO} in WS × C plants. The decreases in ϕ_{NPQ} and increases in ϕ_{NO} likely reflects the inability of the plants to regulate their mechanisms of photoprotection (Yang et al., 2016; Khan et al., 2017; Rios et al., 2017; Urban et al., 2017; dos Reis et al., 2018). Moreover, since ϕ_{NO} corresponds to non-regulated dissipation of excess energy, it can be used as an indicator of the stress-associated risk of reactive oxygen species (ROS) production and photo-damage (Urban et al., 2017; Chen et al., 2018). Consistently, Abid et al. (2018a) showed that severe drought induces ROS formation in wheat. Some damages caused by ROS to the photosynthetic machinery may be long-lasting or irreversibly (Murata et al., 2007; Tikkanen et al., 2014), which is supported by our results (discussed below).

The ability of wheat plants to maintain functions during drought stress and recover after rewatering are dependent on the severity of

Table 8
Mean values of above ground plant's biomass (per pot), number and weight of the grains (per pot), harvest index (HI) and extrapolated 1000 grains weight of wheat plants subjected to different water availability (W), Zn treatments (T) and interaction of W × T. p-values are shown for W, T and W × T. Mean values with different letters (a,b,c) per column indicate statistical significant differences ($p < 0.05$) showed by the Tukey test.

	Plant's biomass (g pot^{-1})	Number of grain (per pot)	Grain weight(g pot^{-1})	HI	Extrapolated 1000 grain weight (g)
Water availability (W)					
Well-watered (WW)	26.45	379.4	12.45	47.0	33.2
Water-stressed (WS)	10.90	132.5	3.63	33.5	28.7
Treatment (T)					
Control (C)	18.68	256.1	7.84	40.2	31.6
Zn priming (ZP)	17.69	241.2	7.21	38.2	30.1
Zn priming + Foliar application (ZPF)	19.67	270.6	9.08	42.4	31.2
W × T					
WW × C	24.73	356.0	11.66	47.8	35.1
WW × ZP	24.90	360.4	10.66	42.9	30.1
WW × ZPF	29.73	421.8	15.04	50.2	34.5
WS × C	12.63	156.2	4.01	32.5	28.1
WS × ZP	10.48	122.0	3.75	33.4	30.1
WS × ZPF	9.60	119.3	3.12	34.5	27.8
p values					
W	< 0.001	< 0.001	< 0.001	< 0.001	0.006
T	0.355	0.495	0.077	0.376	0.670
W × T	0.028	0.143	0.010	0.505	0.088

drought stress (Abid et al., 2018a). Abid et al. (2018a) suggest that if the decrease in photosynthesis during the drought period is mainly attributed to declines in stomatal conductance, rewatering allows for a reversion of these changes and recovery of g_s, A and ϕ_{PSII}. Nonetheless, these authors reported that, after rewatering, plants which had been subjected to severe drought (RWC < 80%) at jointing stage did not completely recover g_s, A and RWC (Abid et al., 2018a). Moreover, photosynthesis in most species may become irreversibly depressed when RWC falls to *c.a.* 70% (Lawlor and Cornic, 2002). In the present study, plants subjected to drought and without any Zn treatment (WS × C) did not completely recuperate A and g_s to levels of WW plants (Fig. 2). The same is true for chlorophyll *a* fluorescence parameters, namely F_v/F_m, ϕ_{PSII}, q_P F'_v/F'_m and ETR (Table 4). These results may not be fully explained by the acceleration of leaf senescence since chlorophyll and carotenoid content did not significantly decreased during the drought period (Table 7). Furthermore, although seven days of watering was sufficient to re-establish a sufficient RWC (> 90%, Table 6), the WS × C plants still appear to be under stress. At 7DWR, WS × C plants presented high values of NPQ (Table 4) and ϕ_{NPQ} (Fig. 3), suggesting the need to dissipate excess energy. These results support the claim that, when low level of RWC are reached during drought, photosynthetic machinery may be irreversibly or long-lasting damage (Lawlor and Cornic, 2002; Parry et al., 2002; Abid et al., 2016).

4.2. Zn treatments enhances photoprotection

Doolette et al. (2018) showed that although limited, the Zn translocation after foliar application of $ZnSO_4$-heptahydrate occurs quickly, under 24 h. In this experiment the time of application and beginning of drought induction was 48 h, which can be considered enough for Zn translocation with the leaf tissues.

Foliar Zn sprays has been reported to cause leaf damage (scorch) under the area where the spray was applied (Doolette et al., 2018). Our group is aware that a higher Zn concentration in a foliar spray would cause visible signs of scorch (unpublished). As such, we selected a concentration where the most of Zn could be theoretical applied to plants without undesirable visible consequences. Here, the upper cuticle tissue thickness (UCT) decreased due to Zn foliar application (Table 5). The cuticle is a crucial barrier that, in concert with stomata, controls plant water status and helps plants survive under drought and high UV radiation (Bi et al., 2017). Furthermore, foliar application of Zn might also induce Zn toxicity in the leaves (Doolette et al., 2018). Signs of metal toxicity include a decrease of the thickness of MT, LET and UET (Atabayeva et al., 2016) as well as the decrease in MXVA, PXVA, PA (de Silva et al., 2012). Moreover, Zn toxicity in leaves can cause a drastic reduction of the net photosynthesis rate by both stomatal limitations as well as reduction in photosynthetic pigments (Vassilev et al., 2011; Atabayeva et al., 2016; Paunov et al., 2018). However, neither ZP or ZPF appear to negatively affect plant's RWC (Table 6), leaf gas exchange (Fig. 2), chlorophyll *a* fluorescence (Table 4) and chlorophyll content (Table 7). Contrastingly, we detected an increase in MT and UET and, consequently, in LT due to zinc foliar application (Table 5). While some authors suggested that Zn might accumulate in MT (Yang et al., 2005), others found no evidence of that (Glińska et al., 2016). Although is known that Zn complexes by ligands in the wheat leaf when $ZnSO_4$ is foliar applied (Doolette et al., 2018), distribution in the leaf tissues are still poorly understood. In any case, we cannot exclude the possibility of Zn accumulation in both UET and MT. Furthermore, as previously said, the increase of LT might allow a higher water use efficiency under drought stress (Izanloo et al., 2008; Abid et al., 2016). The higher values of A/g_s of WS × ZP and WS × ZPF plants, when compared with WS × C, appears to support this claim. In any case, during the drought period, Zn treatments (ZP and ZPF) did not help to maintain higher RWC than on control plants (Table 6).

In the present study, during the drought period, g_s and A were not improved due to either Zn treatments (Fig. 2). Furthermore, only a small increase in F_v/F_m, ϕ_{PSII} and ETR was verified in WS × ZPF when compared with WS × C at 20DD (Table 4). Contrastingly, Karim et al. (2012), which induced terminal drought in wheat, verified an increase in leaf gas exchange in plants were Zn was foliar applied. Complementary, an increase in F_v/F_m in water-stressed wheat due to Zn application was verified in a similar study (Ma et al., 2017). Ma et al. (2017) suggests that Zn may play a protective role in preventing ROS damages in the photosystem machinery by increasing the concentration of antioxidant active substances and, by increasing the transcription and activity of ROS scavenging enzymes.

The observed increase in ϕ_{NPQ}, rather than in ϕ_{NO}, suggests a safe dissipation of absorbed light energy in Zn treated plants subjected to drought (Yang et al., 2016; Khan et al., 2017; Rios et al., 2017; Urban et al., 2017; dos Reis et al., 2018). This contrasted with WS × C plants which presented an increase in ϕ_{NO} (Fig. 3). Similar opposite trends of ϕ_{NPQ} and ϕ_{NO} have also been reported by others (Yang et al., 2016;

Khan et al., 2017). We are not able to discriminate if the increase in ϕ_{NPQ} reduces ROS formation or if the increase in ROS scavenging induced by Zn, as reported by Ma et al. (2017), enables the plant to safely dissipate excess energy. However, since fundamentally all of the plants mechanisms to resist drought are interconnected and complementary to each other (Farooq et al., 2009; Murata et al., 2007; Zargar et al., 2017; Ahmad et al., 2018), we believe that both mechanisms can be acting simultaneously.

As suggested by others, the increase in NPQ and ϕ_{NPQ} during drought might allow a faster and completely recovery of the photosystems after water reestablishment (Gallé et al., 2007; Abid et al., 2016). Contrastingly to WS × C, plants subjected to ZP and ZPF treatments presented a fast recovery of g_s, A and F_v/F_m to non-stressed plants values (Fig. 2; Table 4). A clear recovery of ϕ_{PSII} is also noticeable (Table 4). The reduced unregulated energy dissipation and consequently reduced ROS formations most likely contributed for this feature (Abid et al., 2016).

Submerging seeds in water before sowing is known to improve germination and early growth (Rehman et al., 2015). Since seeds of control plant were submerged in water, we are certain that the effects of priming were due to Zn rather than the initiation of metabolic pathways leading to germination obtained by simply soaking the seeds in an aqueous solution (Bose et al., 2018). It is clear that seed priming (ZP) enhanced photoprotective mechanism in drought-stressed plants, still the combination of priming and foliar application of Zn (ZPF) obtained better outcomes (Fig. 3). Since Zn is required for a wide range of physiological and biochemical processes as well as stress resistance mechanisms (Römheld and Marschner, 1991; Cakmak, 2000, 2005; Hafeez et al., 2013; Ma et al., 2017), it is conceivable that the increase of Zn content in the plant allows for better stress response. This would justify why a double application of Zn (ZPF) performed better than a single application (ZP). Nonetheless, we cannot exclude the possibility that seed priming might have enhanced resistance to abiotic stress by predisposing the plant for quicker and improved stress response. Seed priming was shown to produce an initial stress-exposure which induces a “priming memory” in the plant, increasing stress tolerance in future situations (Chen and Arora, 2013; Wojtyla et al., 2016; Abid et al., 2018b). As far as we know, this is the first study which hints on which physiological mechanisms are involved in stress tolerance due to Zn priming. Indeed, priming with several substances, including $ZnSO_4$, has proven effective in increasing stress tolerance in several crops (Jisha et al., 2013; Paparella et al., 2015). However, we believe that these applications did not simply bridge a plant's Zn deficiency. It is consensual that increasing Zn concentrations in Zn deficient plants help to increase plant growth, photosynthesis or stress response (Cakmak et al., 1996; Cakmak, 2000, 2005; Sharma et al., 2004; Wu et al., 2015). Nevertheless, in our work, well-watered plants (WW), ZP and ZPF did not improved any physiological (Table 4; Figs. 2 and 3) or histological traits (Table 5). Likewise, no harmful physiological consequences of Zn application were observed (Table 4; Figs. 2 and 3). Apart from scorching due to Zn foliar application (Doolette et al., 2018), cytotoxicity and growth impairment have also been reported due to Zn priming (Rehman et al., 2015; Reis et al., 2018). Further optimisation studies can be pursued since in this study we have not tested multiple concentration of Zn for either priming or foliar application. However, we believe that our aim of providing as much Zn as possible to the plants, by either technique, without causing heavy metal toxicity was achieved.

4.3. Genetic instability

The activation of transposable elements (TEs) in plants during stress conditions has been widely reported (Grandbastien, 1998, 2015; Alzohairy et al., 2014; Negi et al., 2016). Some studies suggested that TEs activity, and subsequent genomic alterations constitute a stress response mechanism which may allow phenotypic plasticity and stress adaptation (Grandbastien, 1998, 2015; Negi et al., 2016). On the other hand, other authors proposed that genomic variation may be due to DNA damage caused by ROS (Yigider et al., 2016; Taspinar et al., 2018). Regardless, retrotransposon-based markers, such Inter-Retrotransposon Amplified Polymorphism (IRAP), Retrotransposon-Microsatellite Amplified Polymorphism (REMAP) and Inter-Priming Binding Site (iPBS) have been used to detect instabilities and mutational events derived from RTNs activation (Voronova et al., 2011; Sigmaz et al., 2015; Taspinar et al., 2018). Since induction or genomic alteration may occur in other parts of the plant genome due to TEs activation or DNA damage, other molecular markers not based on retrotransposon have also used to detect polymorphisms caused by abiotic stress (Cenkci et al., 2009; Kekec et al., 2010; Correia et al., 2014). The chromosome structure of wheat, as well as other plant species, consists in gene-rich regions intercalated with intergenic regions where RTNs are dispersed (Sandhu and Gill, 2002). Since RTNs activation is rapidly induced under stress conditions (Alzohairy et al., 2014), the newly appeared and lost bands detected by gene-target molecular markers could arise from RTNs insertion.

In this work, we assessed Genomic Template Stability (GTS) as previously described by others (Correia et al., 2014; Sigmaz et al., 2015; Yigider et al., 2016). Summarily, we considered the polymorphisms detected (gain and/or loss of bands) in stressed plants when compared with control (WW × C). Indeed, a decrease in GTS, assessed by retrotransposon-based and gene-target markers, was observed in plants submitted to drought (Fig. 4). Similarly, Sigmaz et al. (2015) reported an increase in IRAP polymorphism in plants subjected to salinity stress. Likewise, a decrease in GTS was observed in *Pinus sylvestris* submitted to heat stress (Voronova et al., 2011).

Sigmaz et al. (2015) also reported that the use of putrescine could increase GTS since it would alleviate the stress conditions caused by salt stress. Similarly, Yigider et al. (2016) suggested that humid acid caused a decrease of genomic instability caused by manganese stress. With the increase of photoprotective mechanism caused by ZP and ZPF (discussed above), an increase in GTS in WS × ZP and WS × ZPF when compared with WS × C would be expected. However, ZPF appears to decrease GTS in both stressed and non-stressed plants. The increase of concentration of metals like manganese (Yigider et al., 2016) and aluminium (Correia et al., 2014; Taspinar et al., 2018) in the plant's growing medium have been reported to decrease the plant GTS. Moreover, since proteins with zing finger domain are responsible for TEs activation (Jiang et al., 2016), it is possible that the zinc provided by the treatments ZP and ZPF leads to the activation of TEs. Consequently, genetic diversity analysis (Fig. 5) was performed to analyse the influence of drought and Zn treatments in the GTS. Analysis based on genetic similarity have previously showed an obvious genetic distance between Zebra fish exposed to chemical stress and control samples (Zhiyi and Haowen, 2004). Likewise, Gjorgieva et al. (2012) reported that different heavy metals caused distinctly genetic changes in Phaseolus vulgaris RAPD patterns based on genetic similarity analysis. Others, have showed that genetic variation caused by pollutants properly cluster mussel samples submitted to different exposure times, chemicals and experimental scenarios (Qu et al., 2019). Here as previously described (see Results), plants subjected to drought can be clustered together using the x- and y-axis which explain over 80% of genetic variation in either retrotransposon-based and gene-target molecular markers which might indicate distinct genetic alteration caused by drought.

4.4. Biomass production and yield

In Zn-deficient soil, both Zn priming and foliar application have proven effective in increasing wheat yield (Yilmaz et al., 1997; Harris et al., 2008; Gomez-Coronado et al., 2016, 2017). Harris et al. (2008) stated an increase of 14% in grain yield after priming with 0.3% Zn. The combination of priming and foliar application reportedly increased

grain yield by 260% in a study by Yilmaz et al. (1997). In Zn-sufficient conditions, Ma et al. (2017) showed that Zn foliar application was able to increase grain yield by 10%. Contrastingly, Zn foliar application during booting/anthesis did not increase grain yield in a study by Karim et al. (2012). Furthermore, in a study in 23 different experimental sites-years, Zn foliar application induced a slight increase in yield irrespective of the soil and environmental conditions, management practices applied and cultivars (Zou et al., 2012). Seed priming with Zn and/or iron (Fe) was also shown to increase yield parameters in wheat, such as the grain number and yield (Reis et al., 2018). Here, in plants not subjected to drought, ZPF appeared to increase the number of grains with an overall increase of grain weight per pot (Table 8).

Similarly to what reported by Zhang et al. (2018), the number of grains decreased due to drought during anthesis (Table 8). Combined with the decrease in grain weight, overall yield was severely affected by drought (Table 8). The need to increase drought tolerance during anthesis is considered of importance to maintain high yield potentials and greater yield stability of wheat under climate change in Europe (Senapati et al., 2018). A treatment able to improve drought tolerance, delay leaf senescence and extend the plants photosynthetic capacity is expected to increase wheat yield (Izanloo et al., 2008; Semenov et al., 2014). In the present work, however, none of the treatments (ZP or ZPF) was able to mitigate the negative effects of drought in yield (Table 8). It could be expected that alleviating drought stress by enhancement of photoprotective mechanisms would consequently attenuate the loss of yield (Karim et al., 2012; Ma et al., 2017). Accordingly, Karim et al. (2012) suggested that increasing water-use efficiency by foliar application with micronutrients at booting to anthesis can reduce the harmful effects of drought stress. Under terminal drought, these authors reported that Zn foliar application increased grain yield when compared with non-treated plants. Similarly, in rainfed field conditions, foliar application increased grain yield (Ma et al., 2017). Nonetheless, ZP and ZPF did not negatively impact yield and may have increase Zn content in the grain. Although out of the scope of the present work, an increase of bioavailable Zn in the grain due to Zn priming and/or foliar application has been widely reported by others (Yilmaz et al., 1997; Harris et al., 2008; Zou et al., 2012; Gomez-Coronado et al., 2017; Karim et al., 2012; Ma et al., 2017).

5. Final remarks

Severe drought stress induced a non-regulated energy dissipation (ϕ_{NO}) which most likely induced photo-damage and permanently/long lastingly damaged the photosystems. As a consequence, severe drought hindered a full recovery of the plants photosynthetic processes after rewarding. Zinc priming alone (ZP) and/or coupled with foliar application (ZPF) were able to enhance photoprotection during drought by increasing regulated dissipation of excess energy (ϕ_{NPQ}). At the end of the drought period (20DD), ZP and ZPF increased over 2- and 3- fold the ϕ_{NPQ} with an equivalent decrease in ϕ_{NO}. Moreover, Zn treatments enabled a better recovery of wheat plants after stress relief. Due to the severe drought conditions tested in the present study, there was not a clear benefit of Zn treatments in terms of yield of the wheat plants. Nevertheless, this study provided useful insights of the effects of drought/recovery in wheat and the actuation of Zn priming/foliar application.

Author's contribution

IP, JLB and CCorreia conceived and designed the experiment. IP, LR, HF, CCastro, ES and AG maintained the experiment, annotated the plants development and collected the samples. IP, CCorreia and LR acquired leaf gas exchange and chlorophyll *a* fluorescence data. IP and CB prepared the histology slides and performed the tissue measurements and analysis. IP and HF analysed leaf water status and quantified the foliar pigments. JR, AC, and JLB extracted DNA, amplified the molecular markers and assessed genomic stability. IP, LR, HF, CCastro, ES, CB, AG, JLB and CCorreia characterized the plant's morphology and yield. IP and CB made an integrated analysis and discussion of the results. IP was involved in all experimental steps of the study, statistically analysed the results and wrote the paper. CCorreia and JLB provided critical corrections.

Declaration of interest

The authors declare no conflict of interests.

Funding

The authors IP and LR acknowledge their doctoral grants PD/BD/113611/2015, PD/BD/113612/2015, respectively, funded by the FCT under the Doctoral Program “Agricultural Production Chains – from fork to farm” (PD/00122/2012). This work is supported by National Funds by FCT - Portuguese Foundation for Science and Technology, under the project UID/AGR/04033/2019.

Acknowledgements

The authors thank Eng. Coutinho (INIAV-Elvas) for supplying seeds of bread wheat cv. 'Jordão' stored at the Plant Breeding Station at Elvas (Portugal). We thank Mr. Alcídio da Silva for the help in establishing and maintaining the experiments. Furthermore, we thank Mrs. Ana Fraga for her help in preparing the histological slides.

Appendix A. Supplementary data

Supplementary data to this article can be found online at https://doi.org/10.1016/j.plaphy.2019.04.028.

References

Abid, M., Ali, S., Qi, L.K., Zahoor, R., Tian, Z., Jiang, D., Snider, J.L., Dai, T., 2018a. Physiological and biochemical changes during drought and recovery periods at tillering and jointing stages in wheat (*Triticum aestivum* L.). Sci. Rep-UK 8, 4615.

Abid, M., Hakeem, A., Shao, Y., Liu, Y., Zahoor, R., Fan, Y., Suyu, J., Ata-Ul-Karim, S.T., Tian, Z., Jiang, D., Snider, J.L., Dai, T., 2018b. Seed osmopriming invokes stress memory against post-germinative drought stress in wheat (*Triticum aestivum* L.). Environ. Exp. Bot. 145, 12–20.

Abid, M., Tian, Z., Ata-Ul-Karim, S.T., Wang, F., Liu, Y., Zahoor, R., Jiang, D., Dai, T., 2016. Adaptation to and recovery from drought stress at vegetative stages in wheat (*Triticum aestivum*) cultivars. Funct. Plant Biol. 43, 1159–1169.

Acevedo, E.H., Silva, P.C., Silva, H.R., Solar, B.R., 1999. Wheat production in Mediterranean environments. In: Satorre, E.H., Slafer, G.A. (Eds.), Wheat: Ecology and Physiology of Yield Determination. Food Products Press, New York.

Ahmad, Z., Waraich, E.A., Akhtar, S., Anjum, S., Ahmad, T., Mahboob, W., Hafeez, O.B.A., Tapera, T., Labuschagne, M., Rizwan, M., 2018. Physiological responses of wheat to drought stress and its mitigation approaches. Acta Physiol. Plant. 40, 80.

Alzohairy, A.M., Sabir, J.S.M., Gyulai, G., Younis, R.A.A., Jansen, R.K., Bahieldin, A., 2014. Environmental stress activation of plant long-terminal repeat retrotransposons. Funct. Plant Biol. 41, 557–567.

Atabayeva, S., Nurmahanova, A., Akhmetova, A., Narmuratova, M., Asrandina, S., Beisenova, A., Alybayeva, R., Lee, T., 2016. Anatomical peculiarities in wheat (*Triticum aestivum* L.) varieties under copper stress. Pakistan J. Bot. 48, 1399–1405.

Barnabás, B., Jäger, K., Fehér, A., 2007. The effect of drought and heat stress on reproductive processes in cereals. Plant Cell Environ. 31, 11–38.

Bento, M., Pereira, H.S., Rocheta, M., Gustafson, P., Viegas, W., Silva, M., 2008. Polyploidization as a retraction force in plant genome evolution: sequence rearrangements in triticale. PLoS One 3, e1402.

Bi, H., Kovalchuk, N., Langridge, P., Tricker, P.J., Lopato, S., Borisjuk, N., 2017. The impact of drought on wheat leaf cuticle properties. BMC Plant Biol. 17, 85.

Bilger, W., Schreiber, U., 1986. Energy-dependent quenching of dark-level chlorophyll fluorescence in intact leaves. Photosynth. Res. 10, 303–308.

Bose, B., Kumar, M., Singhal, R.K., Mondal, S., 2018. Impact of seed priming on the modulation of physico-chemical and molecular processes during germination, growth, and development of crops. In: Rakshit, A., Singh, H.B. (Eds.), Advances in Seed Priming. Springer Singapore, Singapore, pp. 23–40.

Boyko, A., Kovalchuk, I., 2011. Genome instability and epigenetic modification - heritable responses to environmental stress? Curr. Opin. Plant Biol. 14, 260–266.

Brito, C., Dinis, L.-T., Meijón, M., Ferreira, H., Pinto, G., Moutinho-Pereira, J., Correia, C., 2018. Salicylic acid modulates olive tree physiological and growth responses to drought and rewatering events in a dose dependent manner. J. Plant Physiol. 230, 21–32.

Brodribb, T.J., Holbrook, N.M., 2003. Stomatal closure during leaf dehydration, correlation with other leaf physiological traits. Plant Physiol. 132, 2166.
Brown, P.H., Cakmak, I., Zhang, Q., 1993. Form and function of zinc plants. In: Robson, A.D. (Ed.), Zinc in Soils and Plants: Proceedings of the International Symposium on 'Zinc in Soils and Plants' Held at the University of Western Australia, 27–28 September, 1993. Springer Netherlands, Dordrecht, pp. 93–106.
Cabo, S., Carvalho, A., Rocha, L., Martin, A., Lima-Brito, J., 2014a. IRAP, REMAP and ISSR Fingerprinting in Newly Formed Hexaploid Tritordeum (X *Tritordeum* Ascherson et Graebner) and Respective Parental Species. Plant Mol. Biol. Rep. 32, 761–770.
Cabo, S., Ferreira, L., Carvalho, A., Martins-Lopes, P., Martín, A., Lima-Brito, J., 2014b. Potential of Start Codon Targeted (SCoT) markers for DNA fingerprinting of newly synthesized tritordeums and their respective parents. J. Appl. Genet. 55, 307–312.
Cakmak, I., 2000. Tansley Review No. 111: possible roles of zinc in protecting plant cells from damage by reactive oxygen species. New Phytol. 146, 185–205.
Cakmak, I., 2005. Role of mineral nutrients in tolerance of crop plants to environmental stress factors. In: Proceedings from the International Symposium on Fertigation - Optimizing the Utilization of Water and Nutrients. Sabanci University, Istanbul, Turkey, pp. 35–48.
Cakmak, I., 2008. Enrichment of cereal grains with zinc: agronomic or genetic biofortification? Plant Soil 302, 1–17.
Cakmak, I., Yilmaz, A., Kalayci, M., Ekiz, H., Torun, B., Erenoglu, B., Braun, H.J., 1996. Zinc deficiency as a critical problem in wheat production in Central Anatolia. Plant Soil 180, 165–172.
Carvalho, A., Guedes-Pinto, H., Lima-Brito, J.E., 2012. Genetic diversity in old Portuguese durum wheat cultivars assessed by retrotransposon-based markers. Plant Mol. Biol. Rep. 30, 578–589.
Carvalho, A., Guedes-Pinto, H., Martins-Lopes, P., Lima-Brito, J., 2010. Genetic variability of Old Portuguese bread wheat cultivars assayed by IRAP and REMAP markers. Ann. Appl. Biol. 156, 337–345.
Carvalho, L.C., Coito, J.L., Gonçalves, E.F., Chaves, M.M., Armâncio, S., 2016. Differential physiological response of the grapevine varieties Touriga Nacional and Trincadeira to combined heat, drought and light stresses. Plant Biol. 18.
Cenkci, S., Yıldız, M., Ciğerci, İ.H., Konuk, M., Bozdağ, A., 2009. Toxic chemicals-induced genotoxicity detected by random amplified polymorphic DNA (RAPD) in bean (*Phaseolus vulgaris* L.) seedlings. Chemosphere 76, 900–906.
Chen, K., Arora, R., 2013. Priming memory invokes seed stress-tolerance. Environ. Exp. Bot. 94, 33–45.
Chen, Y.-E., Su, Y.-Q., Zhang, C.-M., Ma, J., Mao, H.-T., Yang, Z.-H., Yuan, M., Zhang, Z.-W., Yuan, S., Zhang, H.-Y., 2018. Comparison of photosynthetic characteristics and antioxidant systems in different wheat strains. J. Plant Growth Regul. 37, 347–359.
Chinnusamy, V., Zhu, J.-K., 2009. Epigenetic regulation of stress responses in plants. Curr. Opin. Plant Biol. 12, 133–139.
Catálogo Nacional de Variedades, 2018. Direção Geral de Alimentação e Veterinária. Agricultura, Florestas e Desenvolvimento Rural. República Portuguesa, pp. 19 ISSN 0871-0295.
Collard, B.C.Y., Mackill, D.J., 2009a. Conserved DNA-derived polymorphism (CDDP): a simple and novel method for generating DNA markers in plants. Plant Mol. Biol. Rep. 27, 558.
Collard, B.Y., Mackill, D., 2009b. Start codon targeted (SCoT) polymorphism: a simple, novel DNA marker technique for generating gene-targeted markers in plants. Plant Mol. Biol. Rep. 27, 86–93.
Correia, S., Matos, M., Ferreira, V., Martins, N., Gonçalves, S., Romano, A., Pinto-Carnide, O., 2014. Molecular instability induced by aluminum stress in Plantago species. Mutat. Res. Genet. Toxicol. 770, 105–111.
Daryanto, S., Wang, L., Jacinthe, P.-A., 2016. Global synthesis of drought effects on maize and wheat production. PLoS One 11, e0156362.
de Silva, N.D.G., Cholewa, E., Ryser, P., 2012. Effects of combined drought and heavy metal stresses on xylem structure and hydraulic conductivity in red maple (*Acer rubrum* L.). J. Exp. Bot. 63, 5957–5966.
Dolferus, R., Ji, X., Richards, R.A., 2011. Abiotic stress and control of grain number in cereals. Plant Sci. 181, 331–341.
Doolette, C.L., Read, T.L., Li, C., Scheckel, K.G., Donner, E., Kopittke, P.M., Schjoerring, J.K., Lombi, E., 2018. Foliar application of zinc sulphate and zinc EDTA to wheat leaves: differences in mobility, distribution, and speciation. J. Exp. Bot. 69, 4469–4481.
dos Reis, C.O., Magalhães, P.C., Avila, R.G., Almeida, L.G., Rabelo, V.M., Carvalho, D.T., Cabral, D.F., Karam, D., de Souza, T.C., 2018. Action of N-succinyl and N,O-dicarboxymethyl chitosan derivatives on chlorophyll photosynthesis and fluorescence in drought-sensitive maize. J. Plant Growth Regul. 1–12 (First Online: 31 October 2018).
Doyle, J.J., Doyle, J.L., 1987. A rapid DNA isolation procedure for small quantities of fresh leaf tissue. Phytochem. Bull. 19, 11–15.
El-Afry, M.M., El-Nady, M.F., Abdelmonteleb, E.B., Metwaly, M.M.S., 2012. Anatomical studies on drought-stressed wheat plants (*Triticum aestivum* L.) treated with some bacterial strains. Acta Biol. Szeged. 56, 165–174.
Fahad, S., Bajwa, A.A., Nazir, U., Anjum, S.A., Farooq, A., Zohaib, A., Sadia, S., Nasim, W., Adkins, S., Saud, S., Ihsan, M.Z., Alharby, H., Wu, C., Wang, D., Huang, J., 2017. Crop production under drought and heat stress: plant responses and management options. Front. Plant Sci. 8.
Farooq, M., Hussain, M., Siddique, K.H.M., 2014. Drought stress in wheat during flowering and grain-filling periods. Crit. Rev. Plant Sci. 33, 331–349.
Farooq, M., Wahid, A., Kobayashi, N., Fujita, D., Basra, S.M.A., 2009. Plant drought stress: effects, mechanisms and management. Agron. Sustain. Dev. 29, 185–212.
Flexas, J., Medrano, H., 2002. Drought-inhibition of photosynthesis in C3 plants: stomatal and non-stomatal limitations revisited. Ann. Bot. (Lond.) 89, 183–189.
Gallé, A., Haldimann, P., Feller, U., 2007. Photosynthetic performance and water relations in young pubescent oak (*Quercus pubescens*) trees during drought stress and recovery. New Phytol. 174, 799–810.
Genty, B., Briantais, J.-M., Baker, N.R., 1989. The relationship between the quantum yield of photosynthetic electron transport and quenching of chlorophyll fluorescence. Biochim. Biophys. Acta Gen. Subj. 990, 87–92.
Gjorgieva, D., Kadifkova-Panovska, T., Mitrev, S., Kovacevik, B., Kostadinovska, E., Baceva, K., Stafilov, T., 2012. Assessment of the genotoxicity of heavy metals in *Phaseolus vulgaris* L. as a model plant system by Random amplified Polymorphic DNA (RAPD) analysis. J. Environ Sci. Health A 47, 366–373.
Glińska, S., Gapińska, M., Michlewska, S., Skiba, E., Kubicki, J., 2016. Analysis of Triticum aestivum seedling response to the excess of zinc. Protoplasma 253, 367–377.
Gomez-Coronado, F., Poblaciones, M.J., Almeida, A.S., Cakmak, I., 2016. Zinc (Zn) concentration of bread wheat grown under Mediterranean conditions as affected by genotype and soil/foliar Zn application. Plant Soil 401, 331–346.
Gomez-Coronado, F., Poblaciones, M.J., Almeida, A.S., Cakmak, I., 2017. Combined zinc and nitrogen fertilization in different bread wheat genotypes grown under Mediterranean conditions. Cereal Res. Commun. 45, 154–165.
Grandbastien, M.-A., 1998. Activation of plant retrotransposons under stress conditions. Trends Plant Sci. 3, 181–187.
Grandbastien, M.-A., 2015. LTR retrotransposons, handy hitchhikers of plant regulation and stress response. Biochim. Biophys. Acta-Gene. Regul. Mech. 1849, 403–416.
Gururani, Mayank A., Venkatesh, J., Tran, L.S.P., 2015. Regulation of photosynthesis during abiotic stress-induced photoinhibition. Mol. Plant 8, 1304–1320.
Hafeez, B., M, K.Y., Saleem, M., 2013. Role of zinc in plant nutrition- a review. Am. J. Exp. Agric. 3, 374–391.
Harris, D., Rashid, A., Miraj, G., Arif, M., Shah, H., 2007. 'On-farm' seed priming with zinc sulphate solution—a cost-effective way to increase the maize yields of resource-poor farmers. Field Crop. Res. 102, 119–127.
Harris, D., Rashid, A., Miraj, G., Arif, M., Yunas, M., 2008. 'On-farm' seed priming with zinc in chickpea and wheat in Pakistan. Plant Soil 306, 3–10.
He, G.-H., Xu, J.-Y., Wang, Y.-X., Liu, J.-M., Li, P.-S., Chen, M., Ma, Y.-Z., Xu, Z.-S., 2016. Drought-responsive WRKY transcription factor genes TaWRKY1 and TaWRKY33 from wheat confer drought and/or heat resistance in Arabidopsis. BMC Plant Biol. 16, 116.
Hendrickson, L., Furbank, R.T., Chow, W.S., 2004. A simple alternative approach to assessing the fate of absorbed light energy using chlorophyll fluorescence. Photosynth. Res. 82, 73.
Huang, C.R.L., Burns, K.H., Boeke, J.D., 2012. Active transposition in genomes. Annu. Rev. Genet. 46, 651–675.
Hussain, S., Maqsood, M.A., Rengel, Z., Aziz, T., 2012. Biofortification and estimated human bioavailability of zinc in wheat grains as influenced by methods of zinc application. Plant Soil 361, 279–290.
Izanloo, A., Condon, A.G., Langridge, P., Tester, M., Schnurbusch, T., 2008. Different mechanisms of adaptation to cyclic water stress in two South Australian bread wheat cultivars. J. Exp. Bot. 59, 3327–3346.
Jaleel, C.A., Manivannan, P., Wahid, A., Farooq, M., Al-Juburi, H.J., Somasundaram, R., Panneerselvam, R., 2009. Drought stress in plants: a review on morphological characteristics and pigments composition. Int. J. Agric. Biol. 11, 100–105.
Jiang, X.-Y., Hou, F., Shen, X.-D., Du, X.-D., Xu, H.-L., Zou, S.-M., 2016. The N-terminal zinc finger domain of Tgf2 transposase contributes to DNA binding and to transposition activity. Sci. Rep-UK 6, 27101.
Jisha, K.C., Vijayakumari, K., Puthur, J.T., 2013. Seed priming for abiotic stress tolerance: an overview. Acta Physiol. Plant. 35, 1381–1396.
Kalendar, R., Antonius, K., Smýkal, P., Schulman, A.H., 2010. iPBS: a universal method for DNA fingerprinting and retrotransposon isolation. Theor. Appl. Genet. 121, 1419–1430.
Kalendar, R., Grob, T., Regina, M., Suoniemi, A., Schulman, A., 1999. IRAP and REMAP: two new retrotransposon-based DNA fingerprinting techniques. Theor. Appl. Genet. 98, 704–711.
Karim, M.R., Zhang, Y.-Q., Zhao, R.-R., Chen, X.-P., Zhang, F.-S., Zou, C.-Q., 2012. Alleviation of drought stress in winter wheat by late foliar application of zinc, boron, and manganese. J. Plant Nutr. Soil Sci. 175, 142–151.
Kekec, G., Sakcali, M.S., Uzonur, I., 2010. Assessment of genotoxic effects of boron on wheat (*Triticum aestivum* L.) and bean (*Phaseolus vulgaris* L.) by using RAPD analysis. Bull. Environ. Contam. Toxicol. 84, 759–764.
Khan, F., Upreti, P., Singh, R., Shukla, P.K., Shirke, P.A., 2017. Physiological performance of two contrasting rice varieties under water stress. Physiol. Mol. Biol. Plants 23, 85–97.
Koressaar, T., Remm, M., 2007. Enhancements and modifications of primer design program Primer3. Bioinformatics 23, 1289–1291.
Krause, G.H., Weis, E., 1991. Chlorophyll fluorescence and photosynthesis: the basics. Annu. Rev. Plant Physiol. 42, 313–349.
Laity, J.H., Lee, B.M., Wright, P.E., 2001. Zinc finger proteins: new insights into structural and functional diversity. Curr. Opin. Struct. Biol. 11, 39–46.
Lawlor, D.W., Cornic, G., 2002. Photosynthetic carbon assimilation and associated metabolism in relation to water deficits in higher plants. Plant Cell Environ. 25, 275–294.
Leff, B., Ramankutty, N., Foley, J.A., 2004. Geographic distribution of major crops across the world. Glob. Biogeochem. Cycles 18 (n/a).
Lesk, C., Rowhani, P., Ramankutty, N., 2016. Influence of extreme weather disasters on global crop production. Nature 529, 84.
Liu, H., Zhou, X., Dong, N., Liu, X., Zhang, H., Zhang, Z., 2011. Expression of a wheat MYB gene in transgenic tobacco enhances resistance to *Ralstonia solanacearum*, and to drought and salt stresses. Funct. Integr. Genom. 11, 431–443.
Lu, C., Zhang, J., 1999. Effects of water stress on photosystem II photochemistry and its thermostability in wheat plants. J. Exp. Bot. 50, 1199–1206.
Luo, M., Liu, X., Singh, P., Cui, Y., Zimmerli, L., Wu, K., 2012. Chromatin modifications

and remodeling in plant abiotic stress responses. Biochim. Biophys. Acta-Gene. Regul. Mech. 1819, 129–136.
Ma, D., Sun, D., Wang, C., Ding, H., Qin, H., Hou, J., Huang, X., Xie, Y., Guo, T., 2017. Physiological responses and yield of wheat plants in zinc-mediated alleviation of drought stress. Front. Plant Sci. 8.
Makarevitch, I., Waters, A.J., West, P.T., Stitzer, M., Hirsch, C.N., Ross-Ibarra, J., Springer, N.M., 2015. Transposable elements contribute to activation of maize genes in response to abiotic stress. PLoS Genet. 11, e1004915.
Murata, N., Takahashi, S., Nishiyama, Y., Allakhverdiev, S.I., 2007. Photoinhibition of photosystem II under environmental stress. BBA-Bioenergetics 1767, 414–421.
Negi, P., Rai, A.N., Suprasanna, P., 2016. Moving through the stressed genome: emerging regulatory roles for transposons in plant stress response. Front. Plant Sci. 7.
Otegui, M.E., Slafer, G.A., 2004. Increasing cereal yield potential by modifying developmental traits. In: Fischer, T., Turner, N., Angus, J., McIntyre, L., Robertson, M., Borrell, A., Lloyd, D. (Eds.), New Directions for a Diverse Planet: Proceedings of the 4th International Crop Science Congress. Crop Science Society of America, Brisbane, Australia.
Ozturk, L., Yazici, M.A., Yucel, C., Torun, A., Cekic, C., Bagci, A., Ozkan, H., Braun, H.-J., Sayers, Z., Cakmak, I., 2006. Concentration and localization of zinc during seed development and germination in wheat. Physiol. Plantarum 128, 144–152.
Paparella, S., Araújo, S.S., Rossi, G., Wijayasinghe, M., Carbonera, D., Balestrazzi, A., 2015. Seed priming: state of the art and new perspectives. Plant Cell Rep. 34, 1281–1293.
Parry, M.A.J., Andralojc, P.J., Khan, S., Lea, P.J., Keys, A.J., 2002. Rubisco activity: effects of drought stress. Ann. Bot. (Lond.) 89, 833–839.
Paunov, M., Koleva, L., Vassilev, A., Vangronsveld, J., Goltsev, V., 2018. Effects of different metals on photosynthesis: cadmium and zinc affect chlorophyll fluorescence in durum wheat. Int. J. Mol. Sci. 19, 787.
Peakall, R.O.D., Smouse, P.E., 2006. Genalex 6: genetic analysis in Excel. Population genetic software for teaching and research. Mol. Ecol. Notes 6, 288–295.
Qu, M., Ding, J., Wang, Y., Chen, S., Zhang, Y., Di, Y., 2019. Genetic impacts induced by BaP and Pb in *Mytilus coruscus*: can RAPD be a validated tool in genotoxicity evaluation both in vivo and in vitro. Ecotoxicol. Environ. Saf. 169, 529–538.
Queen, R.A., Gribbon, B.M., James, C., Jack, P., Flavell, A.J., 2004. Retrotransposon-based molecular markers for linkage and genetic diversity analysis in wheat. Mol. Genet. Genom. 271, 91–97.
Rehman, A., Farooq, M., Ahmad, R., Basra, S.M.A., 2015. Seed priming with zinc improves the germination and early seedling growth of wheat. Seed Sci. Technol. 43, 262–268.
Reis, S., Pavia, I., Carvalho, A., Moutinho-Pereira, J., Correia, C., Lima-Brito, J., 2018. Seed priming with iron and zinc in bread wheat: effects in germination, mitosis and grain yield. Protoplasma 255, 1179–1194.
Rios, J.A., Rios, V.S., Aucique-Pérez, C.E., Cruz, M.F.A., Morais, L.E., DaMatta, F.M., Rodrigues, F.A., 2017. Alteration of photosynthetic performance and source - sink relationships in wheat plants infected by *Pyricularia oryzae*. Plant Pathol. 66, 1496–1507.
Römheld, V., Marschner, H., 1991. Function of micronutrients in plants. In: Mortvedt, J.J., Cox, F.R., Shuman, L.M., Welch, R.M. (Eds.), Micronutrients in Agriculture. Soil Science Society of America, Madison, USA, pp. 297–329.
Saeidi, H., Rahiminejad, M.R., Heslop-Harrison, J.S., 2008. Retroelement insertional polymorphisms, diversity and phylogeography within diploid, D-genome *Aegilops tauschii* (Triticeae, Poaceae) sub-taxa in Iran. Ann. Bot. (Lond.) 101, 855–861.
Sandhu, D., Gill, K.S., 2002. Gene-containing regions of wheat and the other grass genomes. Plant Physiol. 128, 803.
Semenov, M.A., Stratonovitch, P., Alghabari, F., Gooding, M.J., 2014. Adapting wheat in Europe for climate change. J. Cereal Sci. 59, 245–256.
Senapati, N., Stratonovitch, P., Paul, M.J., Semenov, M.A., 2018. Drought tolerance during reproductive development is important for increasing wheat yield potential under climate change in Europe. J. Exp. Bot. ery226.
Sharma, P.N., Kumar, P., Tewari, R.K., 2004. Early signs of oxidative stress in wheat plants subjected to zinc deficiency. J. Plant Nutr. 27, 451–463.
Shiferaw, B., Smale, M., Braun, H.-J., Duveiller, E., Reynolds, M., Muricho, G., 2013. Crops that feed the world 10. Past successes and future challenges to the role played by wheat in global food security. Food Secur 5, 291–317.
Shirasu, K., Schulman, A.H., Lahaye, T., Schulze-Lefert, P., 2000. A contiguous 66-kb barley DNA sequence provides evidence for reversible genome expansion. Genome Res. 10, 908–915.
Sigmaz, B., Agar, G., Arslan, E., Aydin, M., Taspinar, M.S., 2015. The role of putrescine against the long terminal repeat (LTR) retrotransposon polymorphisms induced by salinity stress in *Triticum aestivum*. Acta Physiol. Plant. 37, 251.
Simova-Stoilova, L., Demirevska, K., Petrova, T., Tsenov, N., Feller, U., 2009. Antioxidative protection and proteolytic activity in tolerant and sensitive wheat (*Triticum aestivum* L.) varieties subjected to long-term field drought. Plant Growth Regul. 58, 107–117.
Sims, D.A., Gamon, J.A., 2002. Relationships between leaf pigment content and spectral reflectance across a wide range of species, leaf structures and developmental stages. Remote Sens. Environ. 81, 337–354.
Taspinar, M.S., Aydin, M., Sigmaz, B., Yagci, S., Arslan, E., Agar, G., 2018. Aluminium-induced changes on DNA damage, DNA methylation and LTR retrotransposon polymorphism in maize. Arabian J. Sci. Eng. 43, 123–131.
Tikkanen, M., Mekala, N.R., Aro, E.-M., 2014. Photosystem II photoinhibition-repair cycle protects Photosystem I from irreversible damage. BBA-Bioenergetics 1837, 210–215.
Untergasser, A., Cutcutache, I., Koressaar, T., Ye, J., Faircloth, B.C., Remm, M., Rozen, S.G., 2012. Primer3 - new capabilities and interfaces. Nucleic Acids Res. 40, e115.
Urban, L., Aarrouf, J., Bidel, L.P.R., 2017. Assessing the effects of water deficit on photosynthesis using parameters derived from measurements of leaf gas exchange and of chlorophyll a fluorescence. Front. Plant Sci. 8 2068-2068.
Vallee, B.L., Falchuk, K.H., 1993. The biochemical basis of zinc physiology. Physiol. Rev. 73, 79–118.
Vassilev, A., Nikolova, A., Koleva, L., Lidon, F., 2011. Effects of excess Zn on growth and photosynthetic performance of young bean plants. J. Phytol. 3, 58–62.
Velu, G., Ortiz-Monasterio, I., Cakmak, I., Hao, Y., Singh, R.P., 2014. Biofortification strategies to increase grain zinc and iron concentrations in wheat. J. Cereal Sci. 59, 365–372.
von Caemmerer, S., Farquhar, G.D., 1981. Some relationships between the biochemistry of photosynthesis and the gas exchange of leaves. Planta 153, 376–387.
Voronova, A., Jansons, A., Rungis, D., 2011. Expression of retrotransposon-like sequences in Scots pine (*Pinus sylvestris*) in response to heat stress. Environ. Exp. Biol. 9, 121–127.
Wang, X., Zeng, J., Li, Y., Rong, X., Sun, J., Sun, T., Li, M., Wang, L., Feng, Y., Chai, R., Chen, M., Chang, J., Li, K., Yang, G., He, G., 2015. Expression of TaWRKY44, a wheat WRKY gene, in transgenic tobacco confers multiple abiotic stress tolerances. Front. Plant Sci. 6.
Wegscheider, E., Benjak, A., Forneck, A., 2009. Clonal variation in pinot noir revealed by S-SAP involving universal retrotransposon-based sequences. Am. J. Enol. Vitic. 60, 104–109.
Wojtyla, Ł., Lechowska, K., Kubala, S., Garnczarska, M., 2016. Molecular processes induced in primed seeds - increasing the potential to stabilize crop yields under drought conditions. J. Plant Physiol. 203, 116–126.
Wu, S., Hu, C., Tan, Q., Li, L., Shi, K., Zheng, Y., Sun, X., 2015. Drought stress tolerance mediated by zinc-induced antioxidative defense and osmotic adjustment in cotton (*Gossypium Hirsutum*). Acta Physiol. Plant. 37, 167.
Yang, N., Wang, C.-L., He, W.-P., Qu, Y.-Z., Li, Y.-S., 2016. Photosynthetic characteristics and effects of exogenous glycine of *Chorispora bungeana* under drought stress. Photosynthetica 54, 459–467.
Yang, X., Feng, Y., He, Z., Stoffella, P.J., 2005. Molecular mechanisms of heavy metal hyperaccumulation and phytoremediation. J. Trace Elem. Med. Biol. 18, 339–353.
Yigider, E., Taspinar, M.S., Sigmaz, B., Aydin, M., Agar, G., 2016. Humic acids protective activity against manganese induced LTR (long terminal repeat) retrotransposon polymorphism and genomic instability effects in *Zea mays*. Plant Gene 6, 13–17.
Yilmaz, A., Ekiz, H., Torun, B., Gultekin, I., Karanlik, S., Bagci, S.A., Cakmak, I., 1997. Effect of different zinc application methods on grain yield and zinc concentration in wheat cultivars grown on zinc-deficient calcareous soils. J. Plant Nutr. 20, 461–471.
Zargar, S.M., Gupta, N., Nazir, M., Mahajan, R., Malik, F.A., Sofi, N.R., Shikari, A.B., Salgotra, R.K., 2017. Impact of drought on photosynthesis: molecular perspective. Plant Gene 11, 154–159.
Zhang, J., Zhang, S., Cheng, M., Jiang, H., Zhang, X., Peng, C., Lu, X., Zhang, M., Jin, J., 2018. Effect of drought on agronomic traits of rice and wheat: a meta-analysis. Int. J. Environ. Res. Public Health 15, 839.
Zhang, Y., Shi, R., Rezaul, K.M., Zhang, F., Zou, C., 2010. Iron and zinc concentrations in grain and flour of winter wheat as affected by foliar application. J. Agric. Food Chem. 58, 12268–12274.
Zhiyi, R., Haowen, Y., 2004. A method for genotoxicity detection using random amplified polymorphism DNA with *Danio rerio*. Ecotoxicol. Environ. Saf. 58, 96–103.
Zou, C.Q., Zhang, Y.Q., Rashid, A., Ram, H., Savasli, E., Arisoy, R.Z., Ortiz-Monasterio, I., Simunji, S., Wang, Z.H., Sohu, V., Hassan, M., Kaya, Y., Onder, O., Lungu, O., Mujahid, M.Y., Joshi, A.K., Zelenskiy, Y., Zhang, F.S., Cakmak, I., 2012. Biofortification of wheat with zinc through zinc fertilization in seven countries. Plant Soil 361, 119–130.